UMTRI-2010-24 NOVEMBER 2009

RIDE QUALITY OF JOINTED CONCRETE PAVEMENTS

STEVEN M. KARAMIHAS

UMTRI
UNIVERSITY OF MICHIGAN
TRANSPORTATION RESEARCH INSTITUTE

Technical Report Documentation Page

1. Report No.	2. Government Accession No.	3. Recipient's Catalog No.
UMTRI-2010-24		

4. Title and Subtitle	5. Report Date
Ride Quality of Jointed Concrete Pavements	November, 2009
	6. Performing Organization Code

7. Author(s)	8. Performing Organization Report No.
Steven M. Karamihas	

9. Performing Organization Name and Address	10. Work Unit No. (TRAIS)
The University of Michigan Transportation Research Institute 2901 Baxter Road Ann Arbor, Michigan 48109	11. Contract or Grant No. DTFH61-03-C-00105

12. Sponsoring Agency Name and Address	13. Type of Report and Period Covered
	14. Sponsoring Agency Code

15. Supplementary Notes

16. Abstract

This report describes an experimental study of the link between the International Roughness Index (IRI) and measurements of ride quality on smooth, jointed Portland cement concrete (PCC) pavements in Michigan. The experiment included simultaneous measurements of longitudinal road profile and accelerations at interfaces between the driver and the host vehicle using two test vehicles. The study included measurements on thirty-two pavement sections on freeways and state trunkline roads.
The study examined the relationship between IRI and statistics that summarize whole-body vibration and point vibration levels defined in International Standard ISO 2631-1.

17. Key Word	18. Distribution Statement
concrete pavements, ride quality, road profiles, International Roughness Index	No restrictions.

19. Security Classif. (of this report)	20. Security Classif. (of this page)	21. No. of Pages	22. Price
Unclassified	Unclassified	51	

Table of Contents

List of Figures

List of Tables

Introduction

This report describes an experimental study of the link between the International Roughness Index (IRI) and measurements of ride quality on smooth, jointed Portland cement concrete (PCC) pavements in Michigan. The experiment included simultaneous measurements of longitudinal road profile and accelerations at interfaces between the driver and the host vehicle on several highway pavement sections using two test vehicles. In support of the ongoing development of profile-based smoothness specifications for concrete pavements, the study specifically examines two statistical relationships within the measured data:

1. The relationship between the IRI and accelerations measured at the interfaces between the driver and the vehicle.
2. The relationship between the core model used in the IRI calculation and an objective measurement of whole-body vibration recommended by the International Organization for Standardization (ISO).

A strong statistical connection would help justify using the IRI as a surrogate for ride quality in pavement smoothness incentive programs. Further, it may permit the association of IRI thresholds with established levels of human reaction to whole-body vibration.

The test program covered 32 pavement sections, and it emphasized smooth PCC. Together, this set of pavements provided a diverse and interesting set of test conditions, because it included several different values of joint spacing. Further, many of the test pavements included strong periodic effects (i.e., roughness with a repeating pattern) associated with joint spacing or string line stake spacing.

Measurements of driver vibration included linear and rotational acceleration at three vehicle/driver interfaces: between the supporting seat and the buttocks, between the supporting seat and the back, and between the floor pan and the right foot. The acceleration measurements are combined to form a whole-body vibration metric using ISO 2631-1.[(1)] This metric, and the underlying measurements, is a standardized form of the objective vibration measurement system used by the automotive industry to benchmark the ride quality of vehicles under development and compare them to competitor vehicles.

The IRI provides an estimate of the overall potential for a road profile to excite vertical vehicle vibrations. However, it is based on a simple vehicle model that is restricted to two degrees of freedom, one speed (80 km/h), a standard set of vehicle properties (the "Golden Car" parameters), and the prediction of one vibration quantity (suspension stroke).[(2)] In this study, the IRI is correlated to vehicle response at a variety of speeds. Further, the testing included two vehicles that may not share the same resonance behavior as the Golden Car model upon which the IRI is based. (Their motion will certainly be much more complicated than the motion predicted by the Golden Car model.) As such, this study also examines modified versions of the IRI in which the

model predicts vertical acceleration of the vehicle "body" at the speed of operation for a given experiment. This is not done to suggest that the IRI itself is in need of modification; rather, this is done to determine the relevance of the Golden Car model for a diverse pair of modern test vehicles.

The study is limited in a number of ways. First, few of the test pavements included significant localized roughness, and the transient vibration caused by localized roughness may bias user perception of a ride experience, particularly on otherwise smooth roads. Second, roughness associated with concrete slab curl and warp in Michigan is not always representative of the rest of the country, since many of the jointed PCC pavements in Michigan are composed of long reinforced slabs. (However, the roads in Michigan provided a variety of input spectra that would have been hard to find elsewhere.) Finally, the experiment included only two test vehicles.

Testing Program

Host Vehicles

The measurements were conducted using two host vehicles: a 2005 Infinity QX56 and a 2003 Nissan Altima VQ35. The Altima carried the road profiler and instrumentation for passenger acceleration measurement from 07-Sept-2006 until 29-Sept-2006. The QX56 provided a host vehicle for the profiler during the site selection process from 26-July-2006 through 14-Aug-2006. It also carried the full set of instrumentation from 14-Aug-2006 until 31-Aug-2006.

In part, these vehicles were used because they were available, having been in use in other studies at UMTRI.[3,4] However, they represent two very different segments of the automobile market: a luxury sport-utility vehicle (SUV) and a midsize sedan. While they vary significantly in overall size, weight, and wheel size, they may not necessarily vary significantly in their dynamic response to road roughness. In particular, they may exhibit resonant motions of the body (primary ride) and wheels (wheel hop and/or axle tramp) at a similar set of frequencies.[5] Ideally, a pair of vehicles for this experiment would have included a larger difference in wheelbase. This would help illustrate the interaction between road features having a characteristic longitudinal dimension, such as curling, with longitudinal axle spacing.

Table 1 provides some key information about the host vehicles and the position of the profiler behind them. Figures 1 and 2 provide photos of the test vehicles.

The Altima test vehicle weighed a total of 1856 kg (4083 lb). This consisted of the base vehicle, having a listed curb weight of 1475 kg (3246 lb); fuel; an 80-kg (175-lb) driver; a 118-kg (249-lb) operator; and approximately 190 kg (418 lb) of instrumentation made up of the profiler, the ride measurement system, and other instrumentation on board for separate data collection efforts. The listed curb weight for the Infinity QX56 was 2544 kg (5597 lbs).

Table 1. Vehicle descriptions.

Vehicle	Infinity QX56	Nissan Altima
VIN Number	5N3AA08C55N801472	1N4BL11E63C287028
Tires	P265/70R18 1145 M-5	P215/55R17 93H M+S
Cold Inflation Pressure (kPa)	240-250	228 (front) 214 (rear)
Wheelbase (mm)	3133	2807
Tire Standing Radius (mm)	390	313
Track Width (mm)	1726	1551
Approximate Tire Contact Width (mm)	192	178
Profiler Footprint, Aft of Rear Axle (mm)	1451	1482
Lateral Height Sensor Spacing (mm)	1526	1513

Figure 1. Instrumented Infinity QX56.

Figure 2. Instrumented Nissan Altima.

Test Conditions

The testing covered 32 pavement sections. Thirty-one of the test sections appeared in live traffic on freeways and state trunkline roads with a speed limit of 112 km/h (70 mi/h). The other test section appeared within a construction zone. Table 2 provides the specific location of each test section. All of these appeared within 150 km of UMTRI, so that the ride measurement crew could perform all of their measurements without an overnight stay. These test sections usually appeared within tangent highway segments. Most of the test sections began at a location with a clear event marker, such as a reference post.

Table 2. Test section locations.

Section	Road	Direction	Lane	Start Marker	Test Speeds (km/h)
01	US-23	NB	Passing	MP 11	104, 120
02	US-23	NB	Driving	MP 14	96, 112
03	US-23	NB	Passing	MP 28	104, 120
04	US-23	SB	Driving	MP 5	96, 112
05	US-23	SB	Passing	MP 9	104, 120
06	US-23	SB	Passing	MP 13	104, 120
07	US-23	SB	Passing	MP 15	104, 120
08	US-23	SB	Passing	MP 29	104, 120
09	M-14	EB	Driving	MP 12	96, 112
10	M-14	WB	Driving	MP 14	96, 112
11	M-14	WB	Passing	MP 12	104, 120
12	I-96	WB	Passing	Near MP 144[1]	104, 120
13	I-96	WB	Passing	MP 140	104, 120
14	I-96	EB	Passing	MP 139	104, 120
15	I-96	EB	Driving	MP 143	96, 112
16	US-23	NB	Driving	MP 56	96, 112
17	US-23	SB	Driving	MP 57	96, 112
18	US-23	NB	Driving	MP 73	96, 112
19	US-23	NB	Passing	MP 76	104, 120
20	US-23	NB	Driving	MP 84	96, 112
21	US-23	SB	Passing	MP 73	104, 120
22	I-75	NB	Passing	MP 136	104, 120
23	I-75	SB	Passing	MP 128	104, 120
24	I-75	SB	Passing	MP 132	104, 120
25	I-94	WB	Driving	MP 106	96, 112
26	I-94	EB	Driving	MP 105	96, 112
27	I-94	EB	Driving	MP 113	96, 112
28	I-94	WB	Driving	MP 125	96, 112
29	I-94	EB	Passing	MP 125	104, 120
30	I-94	WB	Driving	MP 146	96, 112
31	I-96	EB	Passing	Near MP 146[2]	104, 120
32	I-69	NB	Driving	Station 1910+00	32-112

NB — Northbound SB — Southbound EB — Eastbound WB — Westbound

1 This section starts at the Adopt a Highway sign west of MP 144.

2 This section starts at the Adopt a Highway sign west of MP 146.

The testing crew performed ride quality and profile measurement at two speeds on each test section, and attempted to complete three runs at each speed. The crew covered test sections in the driving lane at 96 km/h (60 mi/h) and 112 km/h (70 mi/h) as well as test sections in the passing lane at 104 km/h (65 mi/h) and 120 km/h (75 mi/h). This was true on all the test sections except Section 32. This section was closed to traffic, allowing it to be covered at a wider range of test speeds. Testing of Section 32 included three runs at each speed, ranging from 32 km/h (20 mi/h) to 112 km/h (70 mi/h) in increments of 16 km/h (10 mi/h). Appendix A lists the coverage of each section by valid runs.

Note that all the tests went on for 16 seconds, so the length of pavement covered was not the same in each test. The constant test duration made direct comparison between runs at different speeds on the same pavement section more complicated. However, application of standard methods for comparing riding comfort experiences between tests called for a constant time interval.

Table 3 lists some important properties of the test sections. This group of test sections intentionally included several smooth and very smooth pavements as well as several pavements placed within the past five years or less. For example, half of the test sections had Mean Roughness Index (MRI) values below 1.1 m/km (70 in/mi). The overall group of test sections covered a wide variety of joint spacing values. This included five very old pavements with a joint spacing of 21.3 m (70 ft), seven jointed reinforced pavements with a spacing near 12.3 m (40.5 ft), five jointed reinforced pavements with a spacing near 8.2 m (27 ft), and thirteen jointed plain pavements with a spacing of 4.6 m (15 ft) or less. Two very smooth asphalt surfaces were also included for contrast.

Inspection of power spectral density (PSD) plots showed that nearly all of the jointed PCC test sections exhibited significant roughness concentrated at a specific wavelength. This content often appeared at a wavelength equal to the joint spacing or half of the joint spacing and was usually caused by curl or warp of the PCC slabs. In some cases, the level of spectral content concentrated at a wavelength equal to the slab length was different between visits. This was attributed to cyclic changes in the curling induced by changes in the vertical temperature gradient.

In a few cases, roughness was concentrated around a wavelength not equal to the joint spacing. For example, Section 22 included significant roughness at a wavelength of 15 m (49 ft) and Section 20 included significant roughness at a wavelength of 7.5 m (24.5 ft). This was attributed to stringline sag, but that could not be confirmed. A majority of the test sections exhibited roughness that could be linked to either the joint spacing or the string-line stake spacing. Table 3 lists all wavelengths in which the PSD plots illustrated content that dominated or very strongly affected the overall roughness. Note that when slabs are relatively flat in the center, strong spectral content appears at a wavelength equal to half of the slab length.

Table 3 lists the texture type on each pavement surface. The pavement selection process favored pavements with transverse tining, rather than diamond grinding or longitudinal tining. This was done to mitigate problems with profiler repeatability that might result from the interaction between the narrow height sensor footprint and lateral wander over longitudinal channels.[6,7] Most of the sections with transverse tining had a

nominal groove spacing of 12.7 mm (0.5 in). The exceptions were Section 23, with a spacing of 15.9 mm (0.63 in), and Section 31, with a spacing of 19.1 mm (0.75 in). In the majority of cases, the groove spacing was very consistent. However, the groove spacing was randomized about the nominal value on Sections 04, 26-29, and 31.

Table 3. Test section properties.

Section	MRI (m/km)	Surface Type	Joint Spacing (m)	Texture Type	Wavelength with Strong or Dominant Roughness (m)
01	0.7	JPCC	4.6	TT	2.3
02	0.7	JPCC	4.6	TT	2.3
03	0.5	AC	—	Tight mix	—
04	1.4	JPCC	8.2	TT	8.2
05	1.0	JPCC	8.0	TT	8.0
06	0.9	JPCC	4.5	TT	2.3
07	0.9	JPCC	4.7	TT	2.3
08	0.5	AC	—	Tight mix	—
09	1.5	JPCC	21.3	TT	—
10	1.4	JPCC	21.3	TT	—
11	1.3	JPCC	21.3	DG	—
12	1.0	JPCC	12.4	TT	6.2, 12.4
13	0.9	JPCC	4.5	TT	4.5, 2.3
14	1.5	JPCC	4.5	TT	4.5
15	0.8	JPCC	12.2	TT	6.1
16	1.9	JPCC	21.3	DG	—
17	1.5	JPCC	21.3	DG	—
18	0.7	JPCC	4.0	TT	—
19	1.0	JPCC	3.9	TT	3.9
20	1.0	JPCC	4.4	TT	7.5
21	1.0	JPCC	3.9	TT	2.0, 3.9
22	1.2	JPCC	4.2	TT	15.0
23	0.8	JPCC	7.9	TT	—
24	1.1	JPCC	4.1	TT	—
25	3.5	JPCC	12.3	TT	12.3, 6.2
26	3.8	JPCC	12.3	TT	12.3, 6.2
27	3.1	JPCC	12.3	TT	—
28	1.2	JPCC	8.2	TT	8.2, 4.1
29	1.2	JPCC	8.1	TT	8.1, 4.1
30	1.4	JPCC	11.6-12.8	TT	—
31	1.2	JPCC	11.6-12.8	TT	—
32	1.0	JPCC	4.5	TT	—

AC — Asphalt concrete JPCC — Jointed Portland cement concrete
TT — Transversely tined DG — Diamond ground

Instrumentation

The instrumentation included two independent systems: an inertial profiler and a ride measurement system. Each system included its own laptop computer and data acquisition system (DAS). As described in the "Data Processing" section of this report, these systems did not track time consistently, which complicated the analysis.

Inertial Profiler

The inertial profiler was a custom-built system intended for research-quality measurements of proving-ground roads. It collected six data channels: a laser height sensor and a servo-type accelerometer for each of two wheel tracks, a speed sensor, and a channel for user-entered event markers. The accelerometers were operated with an adjustable range that was set to 2.5 g on very smooth roads and up to 10 g on very rough roads. The left-side height sensor was a Selcom Opticator 2207, and the right-side height sensor was a Selcom SLS 5000. Both height sensors projected laser light with a footprint smaller than 3 mm (0.12 in) in the longitudinal and lateral directions.

The system measured longitudinal distance using a DATRON optical speed sensor. The DATRON unit was a non-contacting sensor that used image correlation to detect relative longitudinal motion. The sensor provided a pulse for each 2 mm (0.079 in) of forward longitudinal distance traveled. The pulses served as triggers for data collection. As such, profile measurements were recorded at an interval of 2 mm (0.079 in). The sensor also provided a reading of forward speed at each step using the known distance traveled and an internal clock.

The event marker functioned by recording a voltage offset whenever the user pressed a button. The profiler was mounted to the host vehicle at a trailer hitch, and included fabricated hardware for adjustment of standoff height and orientation. On this mounting system, the lasers appeared 152 cm (59.8 in) apart. Figures 1 and 2, above, show the test vehicles with the profiler attached.

Ride Measurement

Ride measurement was conducted using a system on loan from an automobile manufacturer. This was a custom system in use for objective measurement of ride quality, employed for new vehicle development and benchmarking of existing products. The system measured accelerations at three vehicle/driver interfaces recommended by ISO 2631-1[(1)], along with other data channels required for a proprietary vehicle ride metric.

The data channels included vertical, longitudinal, and lateral acceleration at three interfaces: (1) the interface between the seat bottom and the driver's buttocks (i.e., the seat/buttock interface), (2) the interface between the seat back and the driver's back (i.e., the seat/back interface), and (3) near the location where the floor contacts the driver's pedal foot (i.e., the floor/foot interface). The system also measured rotational acceleration in pitch (i.e., about the lateral axis) at the seat/buttock interface. Pitch acceleration was derived from two vertically oriented accelerometers that were aligned longitudinally a known distance apart. ISO 2631-1 lists all ten of these data channels within the recommended calculation of an "overall vibration total value" for a seated subject.

All ten of the quantities listed above were measured by servo-type accelerometers with calibration factors traceable to the National Institute of Standards and Technology. These sensors attached to the vehicle in standard positions at the seat and accelerator pedal. The sensors for measurement of acceleration at the floor/foot interface appeared to the left of the accelerator pedal to avoid contact with the driver's foot, and about 305 mm (12 in) rearward of the center of the accelerator pedal.

The driver of the vehicles maintained a consistent vertical and longitudinal seat position throughout the testing. The lower portion of the seat was adjusted so that the surface was tilted 13 degrees upward at the front, and the seat/buttock interface sensors were placed 178 mm (7 in) in front of the seat backrest. The axis system at this location tilted with the seat about the global lateral axis, so that the vertical axis maintained an orientation that was perpendicular to the seat surface. The seat backrest was tilted 24 degrees (backward) from a vertical position, and the seat/back interface sensors were placed 305 mm (12 in) above the seat bottom. The axis system at this location tilted with the seat about the global lateral axis, so that the longitudinal axis maintained an orientation that was perpendicular to the seat back surface. The seat/back and seat/buttock sensors were mounted within pads and covered with tape. Figure 3 shows the seat sensors mounted within the Altima.

Figure 3. Seat sensors in the Nissan Altima.

In addition to the ten channels described above, the system included two piezo-electric accelerometers: one above the left profiler accelerometer and one on the lower

control arm near the front left wheel of each test vehicle. The accelerometer at the front left lower control arm measured vertical and longitudinal acceleration. The accelerometer above the left-side profiler measured vertical acceleration. Comparison to its counterpart in the profiler provided a means of fine-tuning the synchronization between the two systems.

The ride measurement system collected data for 16 seconds per run, regardless of vehicle speed. It stored data at a rate of 256 samples per second.

Test Procedure

At the start of each test day, the operator checked the cold inflation pressure of all four tires and adjusted the pressure to the proper level. The profiler and ride measurement system were powered for 15 minutes or more to allow the sensors to warm up. Afterward, the operator performed a bounce test to verify the operational status of the profiler accelerometers and height sensors. The operator also collected data while the profiler host vehicle was not in motion to make sure that system noise was sufficiently low. After the initial system shakedown was complete, the driver operated the host vehicle for at least 16 km (10 mi) at highway speed to warm up the tires.

The same driver and operator performed all of the data collection. In part, this was required to maintain consistent overall vehicle weight and weight distribution. The driver was selected because, in addition to having significant vehicle testing experience, he weighed approximately 80 kg (175 lbs). This technician was closest to the height and weight that appears in many publications for a "standard" human. (See references 8-11.) Driver weight is particularly important, because the driver and seat together form a dynamic system. Although this system is only loosely coupled to vibrations within the rest of the vehicle, driver weight strongly influences vibrations at interfaces between the driver and the seat. All runs were performed with the fuel tank at least two thirds full.

Testing proceeded at each site in the following sequence:

1. The operator prepared the profiler data acquisition system and the ride measurement system for the coming data collection.
2. The driver approached the road segment of interest, brought the vehicle to the desired test speed, and set cruise control.
3. The operator instigated profiler data collection and put the ride measurement system on stand-by.
4. In advance of the road segment of interest, the driver "relaxed" into a standard position and posture and held the steering wheel with his hands at a standard position.
5. At the point of passing the landmark for the road segment of interest, the operator pressed a triggering button. Pressing this button started data acquisition for the ride measurement system and entered a synchronization pulse into the event marker channel of the road profile measurement system.

6. The driver maintained cruise control, a reasonably consistent position within the lane, a standard position and posture, and a standard hand position on the steering wheel for 16 seconds.
7. After 16 seconds, the ride measurement system emitted an audible signal and automatically terminated data acquisition.
8. The operator terminated road profile data acquisition.
9. Steps 1 through 8 were repeated until all of the desired runs were completed.

In some cases, problems with triggering or problems maintaining the desired speed for 16 seconds in live traffic required some runs to be scrapped and repeated.

With the exception of Section 32, all the measurements were conducted in live traffic. In many cases, measurements covered several nearby test sections within a single loop. For example, the testing crew collected data on Sections 01 and 02 in a trip along northbound US-23 and collected data on Sections 07, 06, 05 and 04 during the return trip along southbound US-23.

Both data acquisition systems required the operator to select the anticipated range needed by the accelerometers (in Step 1). Adjusting the range allowed the operator to obtain better precision on smoother test sections. (Hardware that converts analog signals to digital values determines the number of possible values within the selected range. Reducing the range reduces the discretization interval proportionately.) In some cases, finding the proper values for sensor range required a preliminary run. The operator also set the profile spatial sample interval to 2 mm (0.079 in).

The operator screened the data for obvious errors after each run by viewing the raw sensor signals from the profiler. The ride measurement system also provided an audible warning if it detected any signs of compromised data quality, such as sensor signals that were out of range or unrealistic levels of root mean square (RMS) acceleration.

At the end of each testing day, all data were inspected more carefully. This included routine data quality checks, such as:

- verification of the presence of the event marker in the profile measurement system,
- comparison of profile plots and IRI values with repeat runs and with data from the site selection process,
- inspection of RMS acceleration levels and comparison to values from repeat runs,
- inspection of the recorded speed for consistency over the 16-second test interval, and
- inspection of each data file for sufficient duration (i.e., sufficient distance after the trigger for the profiler and 16 seconds of total time for the ride measurement system).

Data Processing

Profile Computation

Data from the inertial profiler were preprocessed as follows:

- Convert all data channels to consistent units, using mm for height and distance. (For example, acceleration was converted to mm/s^2 and speed was converted to mm/s.)
- Low-pass filter the speed channel with a cutoff "length" of 1 m (3.28 ft). (Note that the speed channel is stored at a constant distance interval. As a result, the filter cutoff is expressed in terms of a wavelength that corresponds to a forward travel distance, rather than a length of time.)
- Generate a "time" channel. This is done by dividing the constant distance step of 2 mm (0.079 in) by the instantaneous (filtered) speed-reading at each step.
- Crop the data to include 8 seconds preceding the first event marker and 24 seconds of data following it. This retains 8 seconds of data before and after the 16 seconds of travel on the section of interest.
- Perform automated quality checks on the data over the 16 seconds of interest, including checks for large changes in speed, lack of a second event marker, excessive noise, values that do not fluctuate at all, and sensor data at the limits of the possible range.

The profiler used in this study did not compute profile in real time. After the preprocessing steps, left and right profiles were calculated independently, using a method similar to the calculation method originally developed by Spangler.[12] The following describes the calculation procedure:

- Convert temporal acceleration to spatial acceleration. (This is done at each step throughout the data by dividing temporal acceleration by the square of speed. In this case, speed was not constant.)
- Detrend the accelerometer signal. This process also removes the mean.
- Integrate the accelerometer signal twice. Each integration is performed using straightforward trapezoidal integration. This step produces a record of profiler vertical motion versus distance.
- Detrend the height sensor signal.
- Combine the height sensor and accelerometer signals to produce an elevation profile.
- High-pass filter the elevation profile. This is done using a sixth-order, cascaded form of a Butterworth filter. The filter passes through the signal in both directions to cancel phase distortion.

Ride Measurement Data Processing

Acceleration data at vehicle/driver interfaces were analyzed as required by ISO 2631-1.[1] This process reduced time series measurements of acceleration versus time to individual values of weighted RMS acceleration for each data channel, a total vibration level for a given interface, and an overall vibration level for the combination of all three interfaces.

Analysis by Channel

Each data channel contained a time series measurement of acceleration for a given vehicle/driver interface in a given direction. ISO 2631-1 recommends calculation of RMS acceleration values after application of frequency weighting functions that emphasize content that affects human comfort most. The weighted RMS values reduce a broad band acceleration signal to a single value that would cause an equivalent discomfort level at a reference frequency on a reference axis at a reference location.[13] The weighting functions themselves roughly approximate the inverse of curves that show the sinusoidal or narrow band vibration level needed at each frequency to cause a constant level of discomfort.[14]

Usually, the weighting functions are applied in the frequency domain after estimation of the PSD functions from raw acceleration signals. This restricts the summary index calculations to RMS. Since other quantities (related to transient vibration) were of interest, weighting functions were applied in the time domain using a series of digital filters instead. Each weighting function required a combination of three or four second-order digital filters, including a Butterworth high-pass filter, a Butterworth low-pass filter, an "acceleration-velocity transition" (low-pass) filter, and an "upward step filter." Table 4 lists the weighting function applied to each data channel. Figures 4 and 5 show the weighting functions graphically.

Table 4. Weighting functions and multiplying factors.

Interface	Direction	Weighting Function	Multiplying Factor
Seat/buttock	Longitudinal	W_d	1.0
	Lateral	W_d	1.0
	Vertical	W_k	1.0
	Pitch	W_e	0.4 (m/rad)
Seat/back	Longitudinal	W_c	0.8
	Lateral	W_d	0.5
	Vertical	W_d	0.4
Floor/foot	Longitudinal	W_k	0.25
	Lateral	W_k	0.25
	Vertical	W_k	0.4

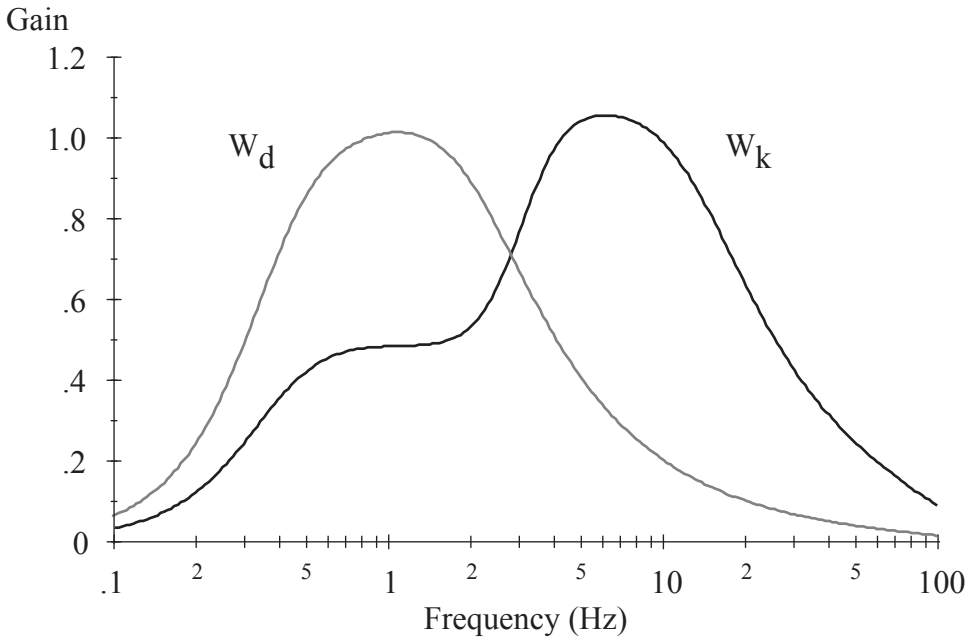

Figure 4. Ride vibration weighting functions.

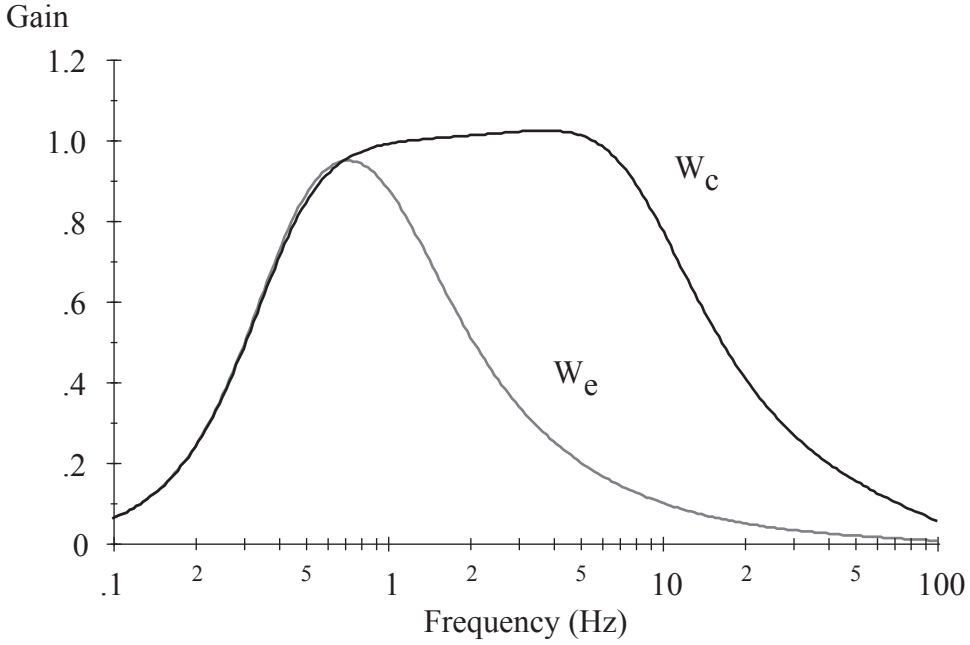

Figure 5. Ride vibration weighting functions.

The frequency responses of these weighting functions reflect the results of several experiments that used laboratory shaker measurements to study the comfort of seated subjects. (See references 15-21.) Weighting function W_k, which is applied to vertical vibration at the seat bottom, emphasizes the frequency range from 4 to 10 Hz. This function is also applied to vibrations at the floor/foot interface in all three directions.

With the exception of longitudinal vibration at the seat/back interface, the weighting functions applied to all other channels emphasize low frequencies.

Once the weighting function is applied to a given channel, quantities such as the RMS value for each channel are calculated directly from the weighted signals in the time domain:

$$a_w = \left[\frac{1}{4096} \sum_{i=1}^{4096} a_w^2(i) \right]^{\frac{1}{2}} \quad (1)$$

Note that the 4,096 samples correspond to a vibration experience 16 seconds long sampled 256 times per second.

Analysis at Each Interface

A "point vibration total value" was calculated for each vehicle/driver interface. The point vibration total value is the root sum of squares of the weighted RMS value in each direction. For the floor/foot interface and seat/back interface, the following defines the point vibration total value:

$$a_v = \left(k_x^2 a_{wx}^2 + k_y^2 a_{wy}^2 + k_z^2 a_{wz}^2 \right)^{\frac{1}{2}} \quad (2)$$

Where x, y, and z represent the longitudinal, lateral, and vertical directions, respectively, and the "k" values are listed in Table 4. The a_v value for the seat/buttock interface also includes a contribution from pitch rotational acceleration. The "k" value for pitch acceleration at the seat/buttock interface is only valid if linear acceleration is expressed in m/sec^2 and rotational acceleration is expressed in rad/sec^2.

Overall Vibration

An "overall vibration total value" was also calculated from the root sum of squares of the point vibration total values from the three vehicle/driver interfaces.

Roughness Index Calculation

Synchronization

Roughness index values covered the range of pavement traversed during the same 16 seconds that the ride measurement system collected data. Since the profiler collected its sensor signals in an independent DAS, the profiler and ride measurement systems were synchronized in post-processing. To help with this, the profiler DAS recorded an event marker at the moment that the ride measurement system began data collection in each run. The delay between the start of ride data collection and the appearance of the event marker was not always the same, but it typically corresponded to about 0.1 m (0.3 ft) of travel distance.

The delay was removed by comparing the measurement of left acceleration from the profiler with a redundant signal collected by the ride measurement system. (The

synchronization was done automatically using cross correlation.) Unfortunately, the two systems did not measure time consistently. The ride measurement system used a clock imbedded within the DAS, and the profiler DAS measured time implicitly by comparing distance and speed. The net result was that, while the shape of common acceleration signals agreed well in each test, one signal often exhibited an increasing level of delay compared to the other. To account for this, the automated synchronization procedure sought the longitudinal distance offset and sample interval adjustment that provided the best agreement between the common channel in both systems.

Typically, the longitudinal distance offset was very small (less than 0.2 m), and the adjustment to the sample interval was less than 0.2 percent. Unfortunately, a linear adjustment to the sample interval failed to line the signals up perfectly because the delay between the signals varied throughout each test. This inconsistency in the latency between the two systems precluded the use of spectral methods to study the statistical dependence of acceleration measurements on profile. Instead, this report seeks to relate summary values of ride vibration to summary roughness indices.

International Roughness Index

All of the profile-based roughness indices examined in this study derive from the IRI and its underlying calculation procedure. The IRI is a general pavement surface condition indicator that was developed to represent a "virtual response-type system" that responded to road profile in a manner very similar to the response-type road roughness measuring systems that were in use at the time of its development.[22] It is based on a simple vehicle model that predicts suspension stroke in response to a single road profile.

The IRI is calculated in four steps.[23]

Step 1: Convert the profile to slope.

Step 2: Apply a 250-mm (9.84 in) moving average.

Step 3: Simulate the response of the "Golden Car" model.

Step 4: Accumulate the average rectified value of suspension stroke, normalized by distance traveled.

Figure 6 illustrates the Golden Car model. The model represents one corner of a vehicle, inasmuch as it predicts the response of one tire and suspension system to a road profile, with the weight supported by the suspension resting over it. This is called a *quarter-car model*. The Golden Car model predicts the response of a quarter-car model, with standard settings for the vehicle properties depicted in Figure 6, to an input profile. The values are:

$m_u/m_s = 0.15$

$k_t/m_s = 653$ (1/sec^2)

$k_s/m_s = 63.3$ (1/sec^2)

$c_s/m_s = 6$ (1/sec)

The IRI is derived from a simulation of the Golden Car that predicts the spatial derivative of suspension stroke at a standard speed of 80 km/h (49.7 mi/h). Note that the moving average base length (B) of 250 mm (9.84 in) is also a standard aspect of the IRI calculation. This is applied before the Golden Car simulation to represent tire envelopment. Reference 24 provides a complete description of the IRI calculation process.

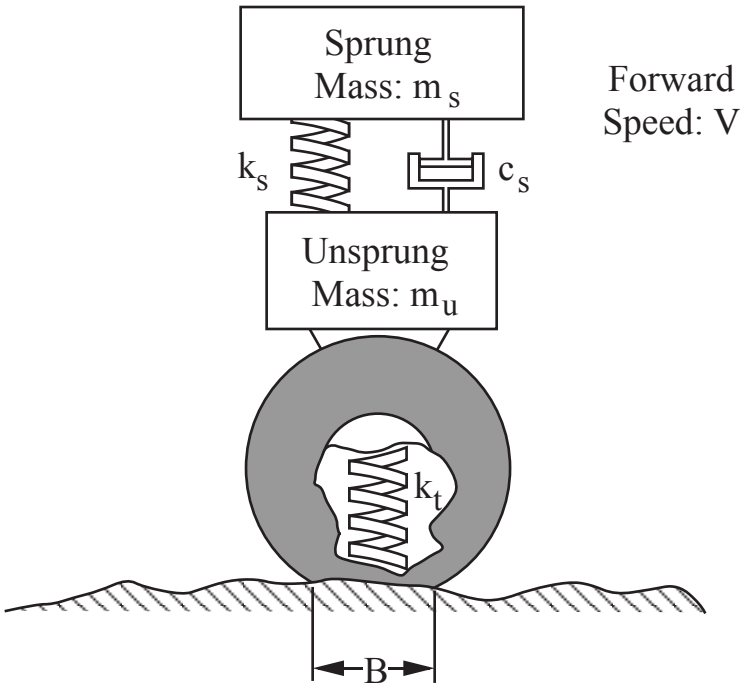

Figure 6. Quarter-car model.[25]

Figure 7 shows the gain function for profile slope of the IRI. Since the Golden Car model uses a fixed speed to calculate the IRI, the gain function may be provided as a function of either temporal frequency (e.g., Hz) or spatial frequency (e.g., wave number in cycles/m). For ease of interpretation, Figure 7 shows gain as a function of wavelength, which is the inverse of wave number. The peak levels of sensitivity occur at wavelengths of 2.30 m (7.55 ft) and 15.78 m (51.8 ft). At a speed of 80 km/h (49.7 mi/h), or 22.2 m/s (72.91 ft/s), the peaks occur at frequencies of 9.66 Hz and 1.41 Hz, respectively. These peaks correspond to resonance frequencies in the Golden Car model, dominated by unsprung mass motion and sprung mass motion, respectively.[23, 26] Overall, the response is above a gain of 0.5 for wavelengths from 1.25 m (4.1 ft) to 30 m (98.4 ft), which correspond to frequencies from 17.8 Hz down to 0.74 Hz at 80 km/h (49.7 mi/h).[22]

This research considered two common "versions" of the IRI.

1. Mean Roughness Index (MRI): This is the average of the IRI from the left side profile and the IRI from the right side profile.
2. Half-car Roughness Index (HRI): This is a two-track version of the IRI, in which left and right side profiles are collapsed to form a single trace before applying the

IRI calculation algorithm. Each point in the collapsed trace is the average of the corresponding points from the left and right side profiles.[27]

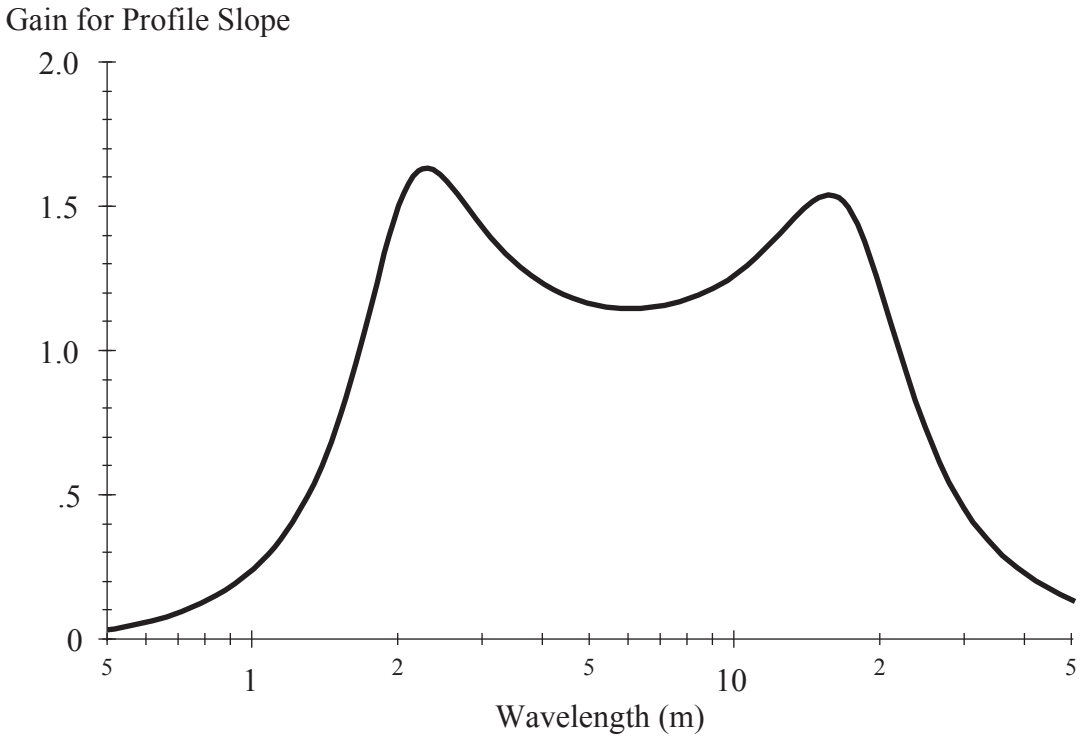

Figure 7. IRI gain for profile slope.

Golden Car Indices

Since the IRI functions as a general pavement-surface condition indicator, it must maintain a reasonable level of relevance to a broad set of performance quantities (suspension stroke, tire loads, passenger acceleration) over a broad range of vehicle types and operating conditions (i.e., speeds). To do this, the IRI calculation algorithm uses several standard settings and provides standard output. That reduces its agreement with specific vibration quantities on specific vehicles but helps maintain its generality.

Seeking to optimize the settings used in the Golden Car model for one aspect of performance on one vehicle compromises the index for others. Nevertheless, this report explores other index options that use the Golden Car model such as: (1) normalizing the vehicle response by time rather than distance traveled, (2) varying the simulated travel speed, (3) reporting the RMS of an output signal rather than the average rectified value, and (4) predicting sprung mass vertical acceleration rather than suspension stroke.

Besides MRI and HRI, this report discusses the relationship between measured acceleration levels in the test vehicles and two other Golden Car indices:

1. Golden Car Average Rectified Suspension Stroking Velocity (GC ARV): This index is calculated by simulating the Golden Car model at the actual test speed, and accumulating the average rectified suspension stroking velocity over a given interval. This index has roots in the original development of the IRI, when

correlation to output from response-type road roughness measurement systems operating at a variety of speeds was important.(28)

2. RMS Golden Car Spring Mass Acceleration (GC ACC): This index provides the RMS value of vertical acceleration of the sprung mass predicted by the Golden Car model at the actual test speed. The "sprung mass" is the mass labeled m_s in Figure 6, above.

Since the speed of each index depends on the test speed, the index will produce one value per test, rather than one value per pavement section. (The simulations ran at the average measured speed for each test, rather than the target test speed, so each test produced an independent index value.)

The examination emphasized a "dual wheel track" version of each index. For GC ARV and GC ACC, the dual wheel track value was the average of the index from the left and right side.

Results

Mean Roughness Index

This section compares MRI values to overall vibration total (OVT) values on the jointed PCC pavements at highway speed. (The analysis excludes the two smooth AC pavements and the lower-speed tests on Section 32.) The data for each vehicle are split into two groups. The first group includes the tests performed with target speeds of 96 km/h (60 mi/h) and 104 km/h (65 mi/h), and the second group includes tests performed with target speeds of 112 km/h (70 mi/h) and 120 km/h (75 mi/h). Data from significantly different speeds were not mixed since the MRI quantifies the intensity of roughness as a function of distance, and the OVT quantifies the intensity of vibrations as a function of time. Further, the vehicles experienced a change in vibration level at each speed. The OVT values for the midsize sedan increased by 2-32 percent with a 16 km/h (10 mi/h) increase in test speed, depending on the test section. The OVT values for the luxury SUV decreased on four of the test sections at the higher speed but increased up to 26 percent on the rest.

Figures 8 and 9 compare vibration level to roughness for the midsize sedan, and Figures 10 and 11 compare them for the luxury SUV. Each figure shows a best-fit line, and provides the RMS residual from the linear fit and the square of the Pearson correlation coefficient (i.e., the coefficient of determination, or R^2). Since the values of MRI are not normally distributed, the RMS residual provides a more appropriate characterization of the correlation level than the coefficient of determination.[1] For example, when values for MRI above 3 m/km (190 in/mi) are removed, the R^2 value for

[1]The coefficient of determination provides a deceptive assessment of the correlation level when the "goodness of fit" benefits from relatively few points with values that are very different from the rest. These data fit that description.

the data depicted in Figure 8 reduces from 0.96 to 0.85, but the RMS residual only reduces from 0.0055 g to 0.0050 g.

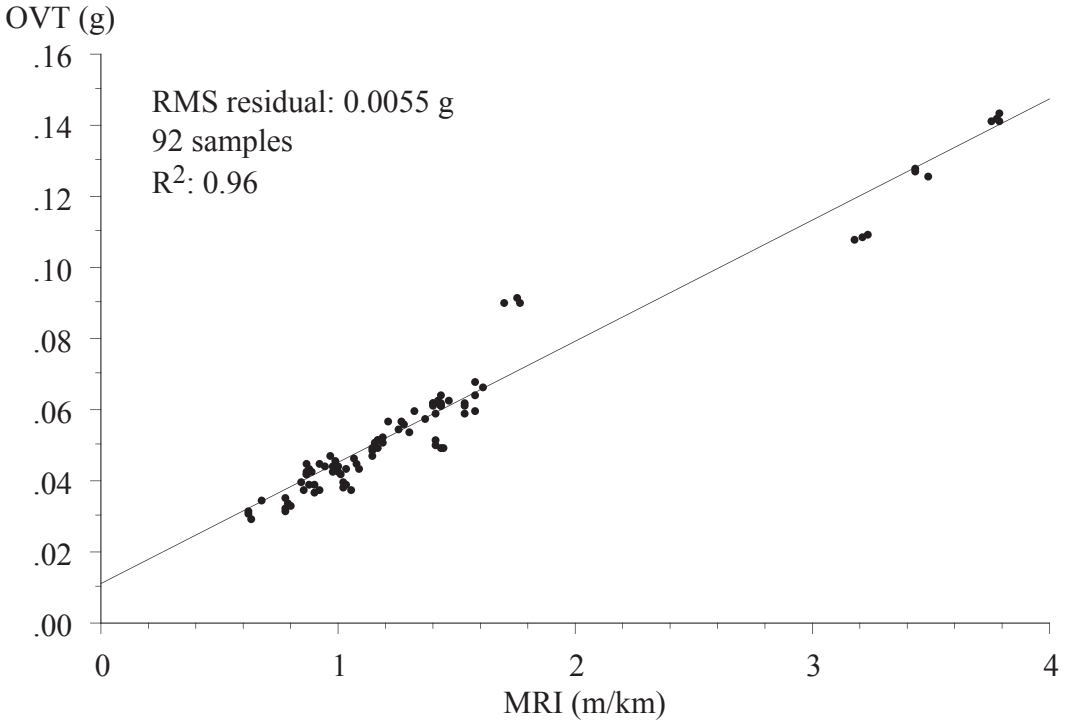

Figure 8. OVT versus MRI, midsize sedan, 96-104 km/h.

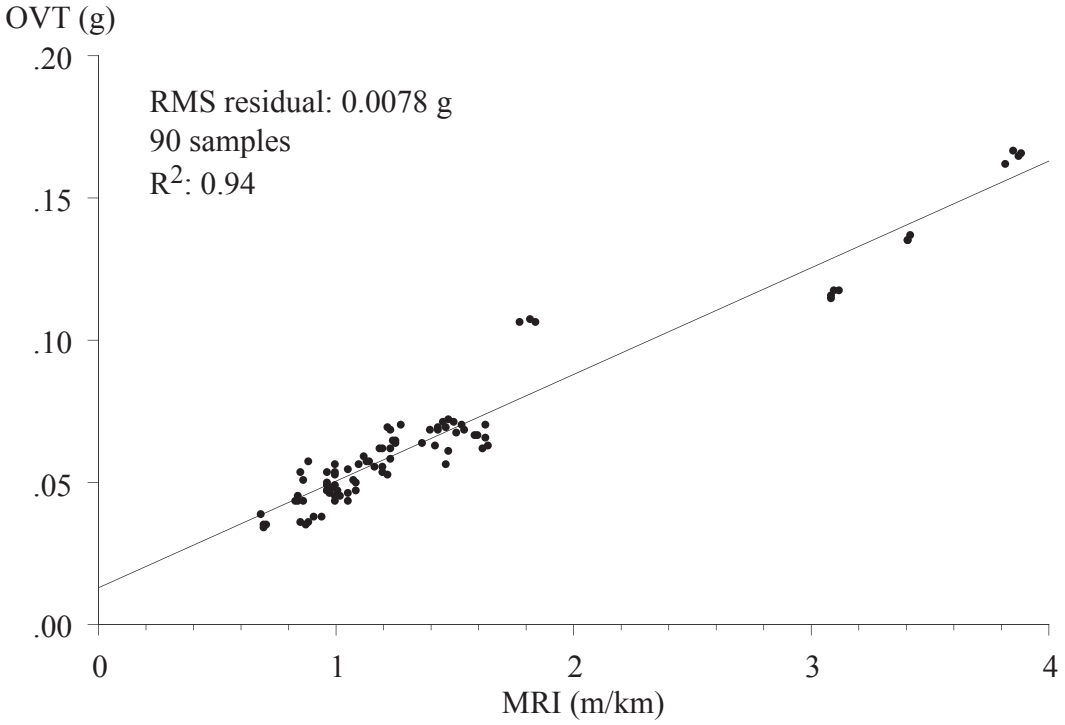

Figure 9. OVT versus MRI, midsize sedan, 112-120 km/h.

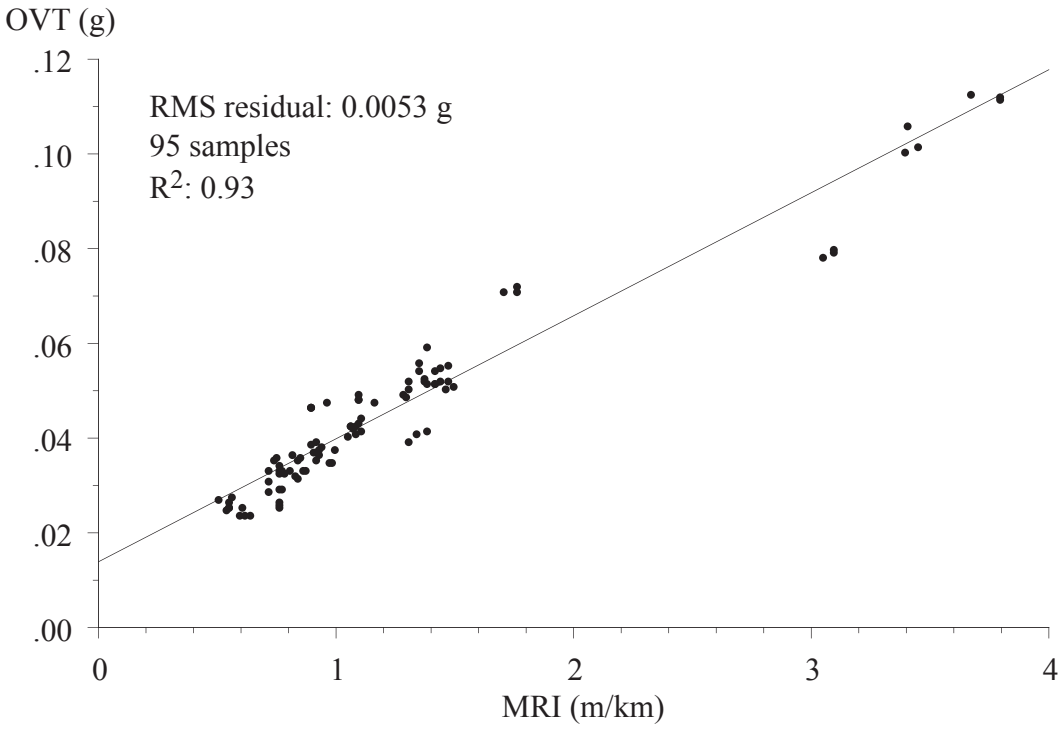

Figure 10. OVT versus MRI, luxury SUV, 96-104 km/h.

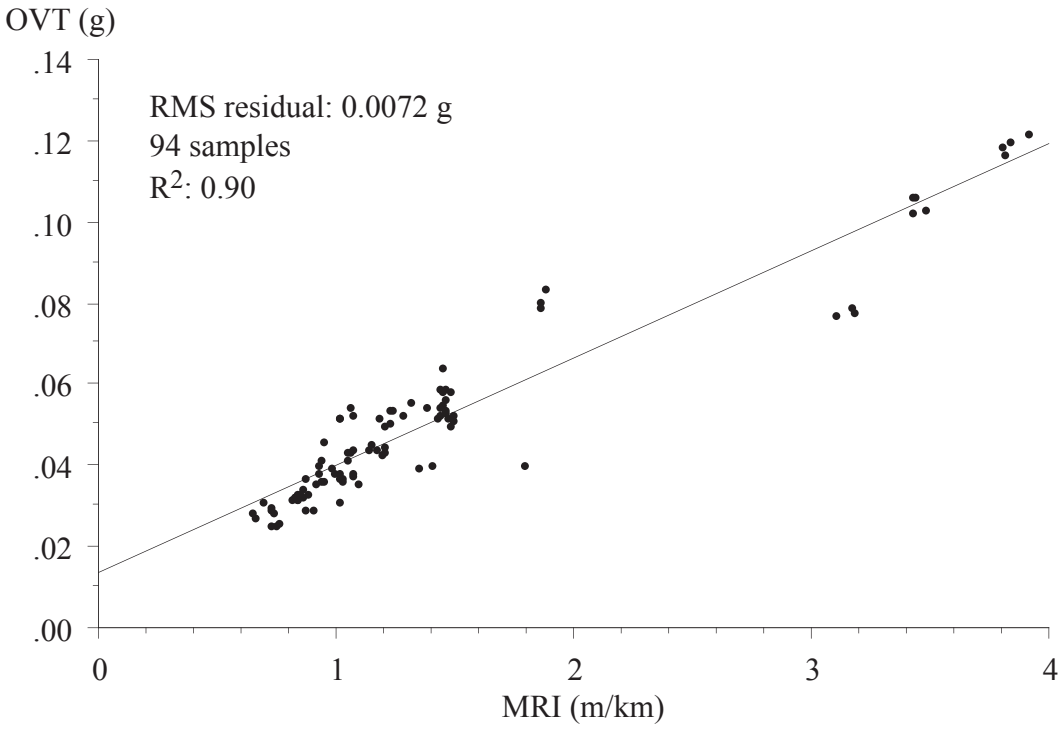

Figure 11. OVT versus MRI, luxury SUV, 112-120 km/h.

Figure 8 cites an RMS residual of 0.0055 g. This is a small absolute acceleration level (0.054 m/s^2), but it is about 5 percent of the overall data range. For example, the 0.0055 g value of RMS residual translated to about 0.16 m/km (10 in/mi) through the slope of the best-fit line. Nevertheless, the relationship between MRI and the overall level of measured vibration is good on both vehicles and at both speeds. The correlation is roughly equal when the HRI replaces MRI and is only slightly degraded for the IRI on either the left or right side. However, these four IRI-based roughness index options are not interchangeable. The similarity between the correlation levels here owes in large part to the fact that longitudinal profiles of smooth PCC pavement often vary little between the left and right side, particularly in the long wavelength range.[29,30] Appendix B lists correlation statistics for comparison of all four IRI-based index options to several vibration quantities.

While the MRI does not provide information directly equivalent to occupant vibration measurements, the high correlation level justifies the effort to reduce IRI-based roughness index values to decrease the vibration experienced by automobile occupants.

In Figures 8 through 11, the best-fit lines all intercept the ordinate axis with a positive value of OVT. Under more heavily controlled measurements, the positive intercept may imply the presence of vibration sources other than road roughness, such as tire imbalance, engine vibration, or aerodynamics. All of these mechanisms cause the vehicle to vibrate while operating in the absence of road roughness. However, the measurements of both road profile and vibration level include some level of sensor noise that affected the MRI and OVT. Without precise knowledge of these noise levels, the implications of the intercept should be interpreted with care. Further, the data at high roughness levels, where vibration from sources other than the profiles are less significant, influenced the y-intercept significantly.

All four plots include three data points from Section 16 with an MRI value near 1.8 m/km (115 in/mi) that have higher vibration levels than expected, given the trend in the rest of the data. In this case, the MRI underestimated the contribution of road roughness to vehicle vibration level. Unlike the rest of the test pavements, long wavelength content dominates the roughness of Section 16. Long wavelength roughness affected the OVT more than the MRI on this pavement because: (1) the tests were performed at a higher speed than the MRI simulation speed, and (2) many of the weighting functions for the vibration measurement channels emphasize low frequency vibrations, which are excited by long wavelength roughness.

A strong relationship was found between MRI and point vibration totals at the each of the three vehicle/driver interfaces. (See Appendix B.) The best relationship was found between MRI and the point vibration total value at the floor/foot interface. For example, the RMS residual value for a linear fit between the floor/foot point vibration total and MRI ranges from 0.007 to 0.014 g, depending on the vehicle and operating speed range. Of the individual channels, RMS vertical vibration at the floor/foot position related to MRI best, and lateral vibration at all three interfaces related to MRI poorly.

For the same test pavement, the OVT values within the luxury SUV were approximately 30-40 percent lower than the values in the midsize sedan at the same operating speed.

MRI Thresholds

ISO 2631-1 specifies ranges of OVT values that correspond to "likely reactions" of passengers in public transport.[1] The overlapping ranges are specified here in units compatible with Figure 8 through 11:

Less than 0.032 g:	not uncomfortable
0.032 g to 0.064 g:	a little uncomfortable
0.051 g to 0.102 g:	fairly uncomfortable
0.082 g to 0.163 g:	uncomfortable
0.127 g to 0.255 g:	very uncomfortable
Greater than 0.204 g:	extremely uncomfortable

Table 5 lists the range of MRI associated with each "likely reaction" for both vehicles at both speed ranges discussed above. The table provides the range of MRI values that correspond to each category by translating each vibration threshold value through the best-fit lines in Figures 8 though 11.

Table 5. MRI ranges (m/km) associated with "likely reactions" to vibration.

Likely Reaction	Midsize vehicle		Luxury SUV	
	96-104 km/h	112-120 km/h	96-104 km/h	112-120 km/h
not uncomfortable	< 0.62	< 0.52	< 0.70	< 0.70
a little uncomfortable	0.62-1.56	0.52-1.37	0.70-1.93	0.70-1.92
fairly uncomfortable	1.18-2.67	1.02-2.38	1.42-3.38	1.42-3.35
uncomfortable	2.07-4.47	1.83-4.01	2.60-5.74	2.58-5.67
very uncomfortable	3.42-7.16	3.06-6.46	4.36-9.27	4.31-9.14
extremely uncomfortable	> 5.66	> 5.10	> 7.31	> 7.21

Setting smoothness thresholds based on these ranges is problematic for four reasons. First, the data only include the response of two vehicles. Second, an acceptable level of road roughness for one vehicle may not be acceptable in another. For example, the luxury SUV produced levels of passenger vibration at a significantly higher roughness level than the midsize sedan. Third, vibration level in a given vehicle is often very sensitive to speed. The results for the midsize sedan listed in Table 5 demonstrate this, since the roughness levels corresponding to each range were 10-16 percent lower at the higher speed. In contrast, the roughness ranges produced by data from the luxury SUV did not change significantly with speed. Fourth, some of the ranges listed above are very broad. In spite of these complications, Table 5 provides useful context for the MRI scale.

At the time this report was written, the Federal Highway Administration's (FHWA) performance goals for smoothness of the National Highway System (NHS) were as follows:

- 58.5 percent of vehicle miles traveled on facilities with a reported IRI of 1.50 m/km (95 in/mi) or less, and
- 95 percent of vehicle miles traveled on facilities with a reported IRI of 2.68 m/km (170 in/mi) or less.

These ranges represent the "good" and "acceptable" categories for NHS pavements, respectively. Table 5 shows that drivers of the two vehicles studied here at highway speed will rarely, if ever, experience a very uncomfortable or extremely uncomfortable vibration experience caused by roughness on a NHS pavement that is deemed "acceptable" by the FHWA. Most of the pavements covered in this study produced a vibration experience in the "not uncomfortable" or "a little uncomfortable" categories within the luxury SUV, and all of the pavements produced a vibration experience classified as "fairly uncomfortable" or better within the midsize sedan.

A recent report by Wilde provides smoothness thresholds in use in 2007 by six states using the IRI.[31] Table 6 summarizes the IRI range for full pay and the IRI value needed to achieve maximum incentive bonus for new PCC pavements in each state. The IRI values for maximum bonus in New Mexico, Pennsylvania, Texas, and Virginia correspond well with the MRI values observed in the two test vehicles at the upper limit for a vibration experience classified as "not uncomfortable." This is a point at which extra effort to decrease roughness may offer little additional ride comfort to the user, as long as the pavement maintains that level of smoothness.

Table 6. IRI thresholds for new PCC.

State	Full Pay Range (m/km)	Maximum Bonus Threshold (m/km)
Kentucky	< 0.84	—
Michigan	< 1.10	—
New Mexico	0.97 - 0.98	0.82
Pennsylvania	0.95 - 1.10	0.55
Texas	0.95 - 1.03	0.49
Virginia	0.87 - 1.10	0.71

When either vehicle traversed pavements that would have earned full pay in these six states, the vibration experience always fell well below the upper limit of the "a little uncomfortable" range. However, at the higher test speed, the vibration level in the midsize sedan overlapped the "fairly uncomfortable" range slightly.

The relationship between current IRI thresholds in place at State and Federal agencies and "likely reactions" to vibration in these two vehicles is encouraging. However, the public's true reaction to road roughness depends heavily on their expectations[1], as well as whether the ride experience includes transient events (i.e., localized roughness).

Tire Imbalance

Inspection of PSD functions from measured acceleration signals revealed that tire imbalance induced significant vibration at the spindles of both vehicles. Accelerations caused by tire imbalance influence accelerations at vehicle/driver interfaces much less than at the spindle. Nevertheless, it caused a significant share of the weighted vertical and longitudinal acceleration on the smoothest roads, particularly at the floor/foot interface. For example, on Section 15 tire imbalance accounted for about 24 percent of the floor/foot vertical acceleration and 37 percent of the longitudinal acceleration at a travel speed of 95 km/h (59 mi/h).

Figures 12 through 15 help illustrate this calculation for a run on Section 15 at 111 km/h (69 mi/h). Figure 12 shows the PSD of left slope from Section 15. (PSD of slope, rather than elevation, are shown here because the response of the IRI algorithm is much more uniform for slope input than elevation. Further, the content of a slope PSD typically covers fewer orders of magnitude than an elevation PSD, so areas of strong content are more obvious.) Spikes appear in the plots at wave numbers of 0.082 cycles/m (0.025 cycles/ft) and 0.164 cycles/m (0.050 cycles/ft), which correspond roughly to wavelengths of 12.2 m (40 ft) and 6.1 m (20 ft), respectively. Upward curling of the 12.2-m (40-ft) long slabs accounts for both of these spikes, where the "upper harmonic" at a wavelength of 6.1 m (20 ft) is caused by the relatively flat shape of the slab. The content at a wavelength of 6.1 m (20 ft) dominates the roughness. (This would be more obvious with log scaling on the ordinate axis.)

Figure 13 shows the PSD of weighted vertical acceleration at the floor/foot interface for a run on Section 15 at about 95 km/h (59 mi/h). Due to the influence of the weighting function, the acceleration level rolls off at very high frequencies and at very low frequencies. The spikes within the PSD plot at 2.13 Hz and 4.25 Hz correspond to wavelengths of 12.3 m (40.5 ft) and 6.2 m (20.3 ft), respectively.[2],[3] These appear because of vehicle vibration response to the curled slabs. However, another significant spike appears in the PSD plot at 10.7 Hz. This corresponds to a wavelength of 2.47 m (8.1 ft).

Since the profile did not include content isolated at a 2.47-m (8.1-ft) wavelength, the acceleration at 10.7 Hz may have been caused by resonance behavior within the vehicle. If so, the spike would appear at the same frequency for tests at other speeds. Figure 14 shows the PSD of weighted vertical acceleration at the floor/foot interface for a run on Section 15 at about 111 km/h (69 mi/h). In this plot, no spike appears at 10.7 Hz. Instead, spikes appear at 2.53 Hz, 5.06 Hz, 12.38 Hz, and 24.76 Hz, which correspond to lengths of 12.2 m (40 ft), 6.1 m (20 ft), 2.49 m (8.2 ft) and 1.24 m (4.1 ft). The first two spikes are again caused by slab curl. The third occurs at the same wavelength as it appeared at the lower speed. In this case, the length corresponds closely to the tire circumference of 2.45 m (8 ft). This suggests wheel imbalance as the cause. The content at 24.76 Hz is an

[2]For example, at the travel speed of 26.4 m/s, the wavelength that corresponds to 2.13 Hz is (26.4 m/s)/(2.13 cycles/s) = 12.3 m/cycle.

[3]The values of wavelength do not match precisely because the PSD plots split the frequency ranges into coarse bins.

upper harmonic of the motion caused by wheel imbalance, which is periodic but not perfectly sinusoidal.

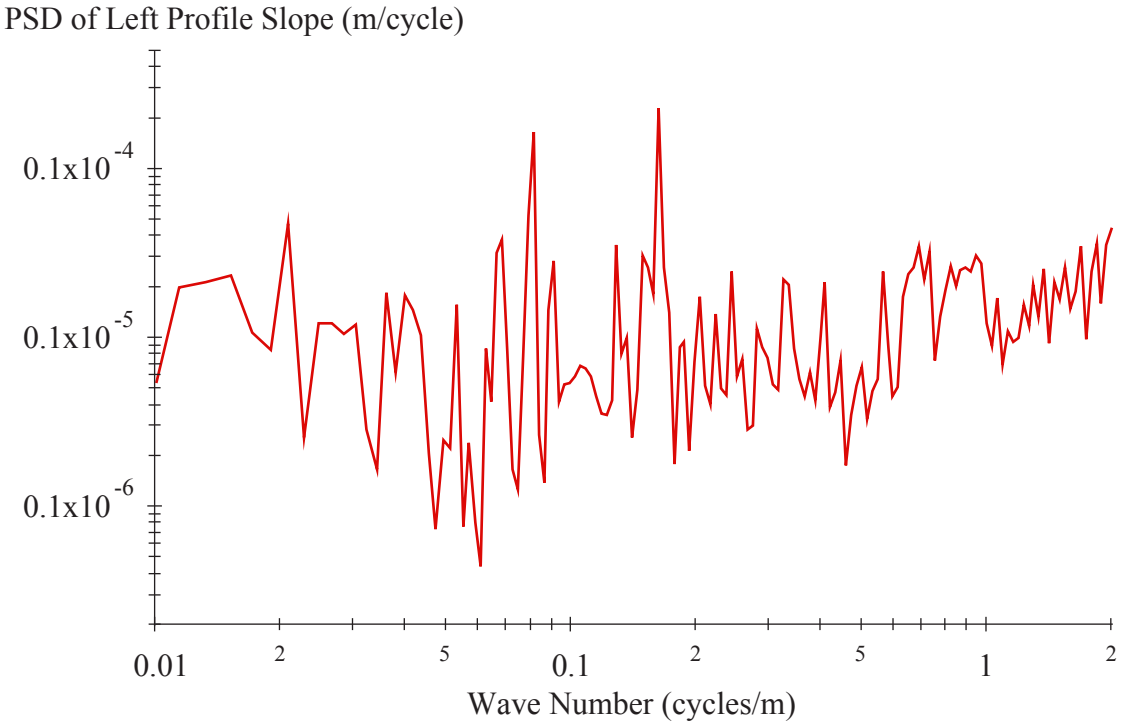

Figure 12. PSD of left profile slope, Section 15.

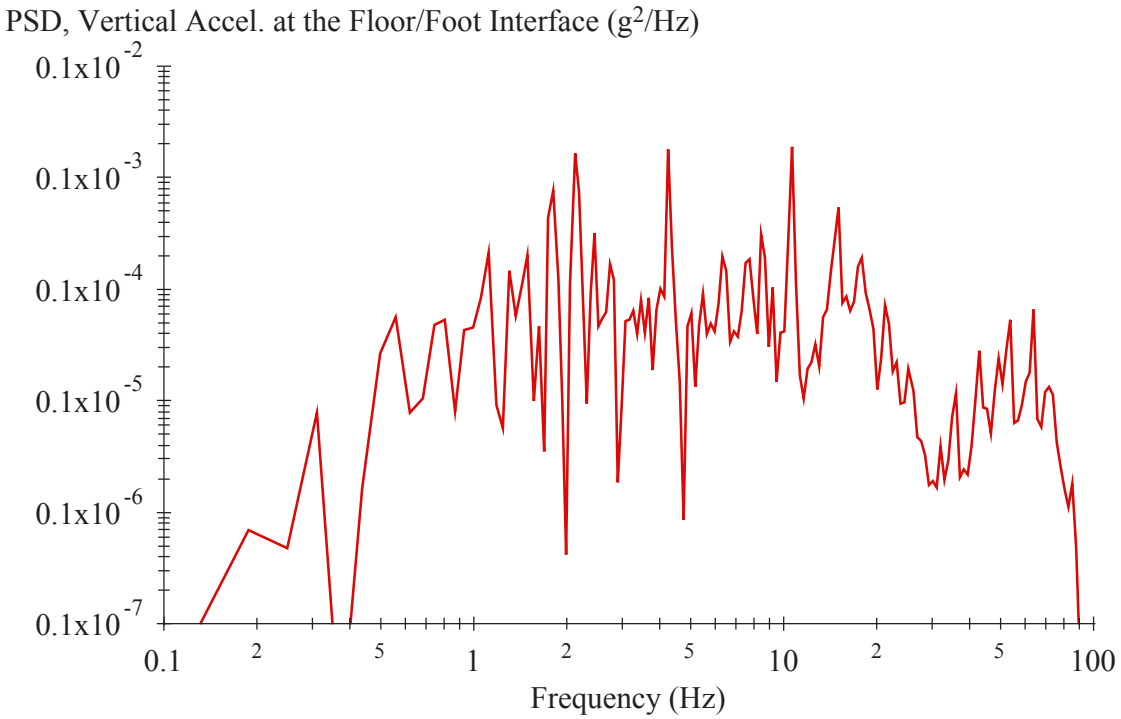

Figure 13. PSD of filtered acceleration on Section 15 at 95 km/h.

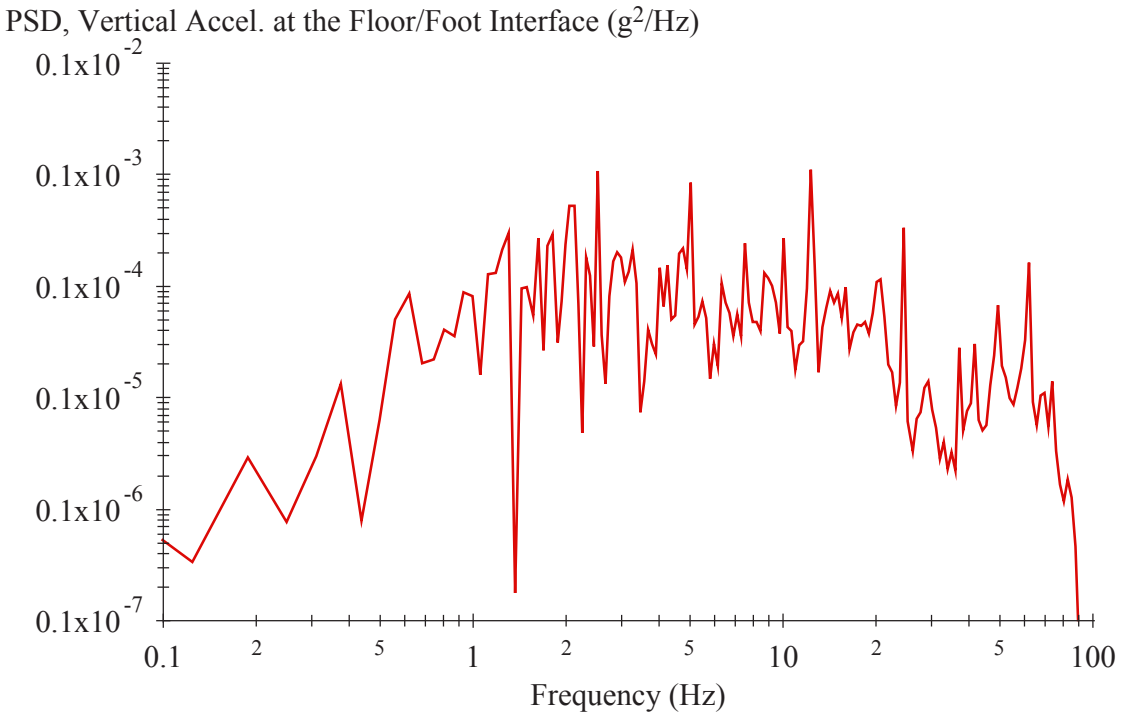

Figure 14. PSD of filtered acceleration on section 15 at 111 km/h.

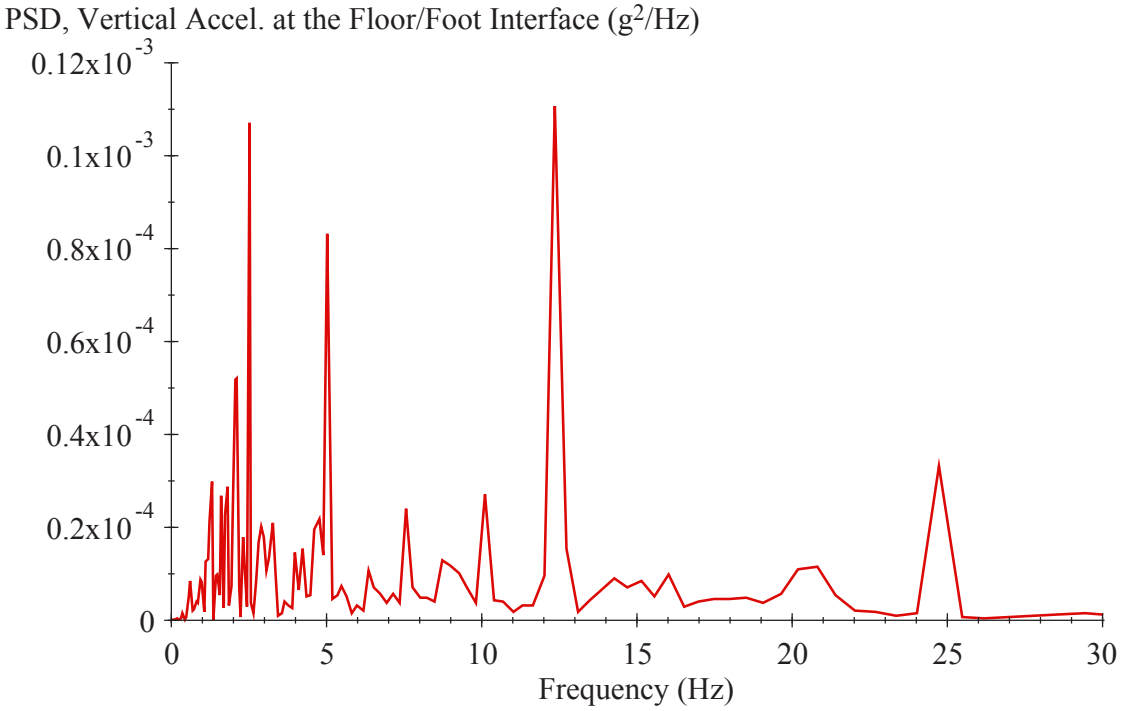

Figure 15. PSD of filtered acceleration on section 15 at 111 km/h, linear scaling.

The PSD plot provides a good demonstration of the way each waveband contributes to RMS acceleration when it is plotted on a linear scale. This is because the mean squared

acceleration level is equal to the area under the PSD plot.[4] Figure 15 shows the PSD from Figure 14 on a linear scale. The four spikes caused by slab curl and tire imbalance stand out much more with linear scaling. In this plot, the spikes at 12.38 Hz and 24.76 Hz alone account for a mean square acceleration level of 2.06×10^{-5} g^2, or an RMS value of 4.54×10^{-3} g. This is 30 percent of the total RMS acceleration value of 1.90×10^{-2} g. A repeat of this analysis for the longitudinal acceleration at the floor/foot interface at this speed shows that tire imbalance accounted for 52 percent of the RMS value.

No special effort was made to balance the tires on either test vehicle. However, the tires were not noticeably out of balance, and much of the imbalance was caused by rocks and other debris held within the tire tread. Although the seat helps isolate the driver from the influence of tire imbalance, it still affects the weighted acceleration levels at the seat/buttock and seat/back interfaces. Further, the effect of tire imbalance dominated acceleration at the steering wheel, particularly in the longitudinal direction.

Golden Car Indices

The results above show that a significant relationship exists between MRI and measured accelerations at vehicle/driver interfaces on the two test vehicles. This owes primarily to the fact that both the MRI and the frequency-weighted acceleration measurements were roughly sensitive to the same range of wavelengths within the road profiles.

The IRI (and hence, the MRI) responds to a broad range of wavelengths that affect vehicle vibration response such as suspension stroke, fluctuations in tire vertical load, and vehicle body acceleration. This is the source of its generality and allows the IRI to provide relevant information for a wide range of applications. However, for the specific job of predicting RMS accelerations at vehicle/driver interfaces and OVT in a specific vehicle, the IRI is restricted in the following ways:

- The IRI describes the vehicle using a "quarter-car" model, which is a relatively simple vehicle model. (See Figure 6.)
- The IRI uses a standard set of vehicle properties, called the "Golden Car" parameters.
- The IRI simulates a vehicle at a standard speed of 80 km/h (49.7 mi/h).
- The IRI normalizes response by distance traveled, rather than time.
- The IRI summarizes roughness using absolute suspension stroke, rather than sprung mass acceleration.

All of these restrictions ensure that the IRI maintains a standard definition and standard meaning for the IRI scale. (See references 23, 24 and 28.) This section of the report explores the relevance of the Golden Car model to measured accelerations at

[4]In this work, the calculation was performed in the time domain instead, but it was checked for accuracy against frequency domain calculations.

vehicle/driver interfaces on the two test vehicles by relaxing the last three restrictions listed above.

Golden Car Average Rectified Velocity

Simulation speed strongly affects the summary roughness value produced by the Golden Car model.[32] Figure 16 shows the variation in average rectified slope (ARS) predicted by the Golden Car model versus speed for Section 32. In this case, the figure shows the mean value from the left and right wheel track. The "mean GC ARS" value is the absolute suspension slope normalized by the distance traveled, and it is equal to the MRI when the simulation speed is 80 km/h (49.7 mi/h).

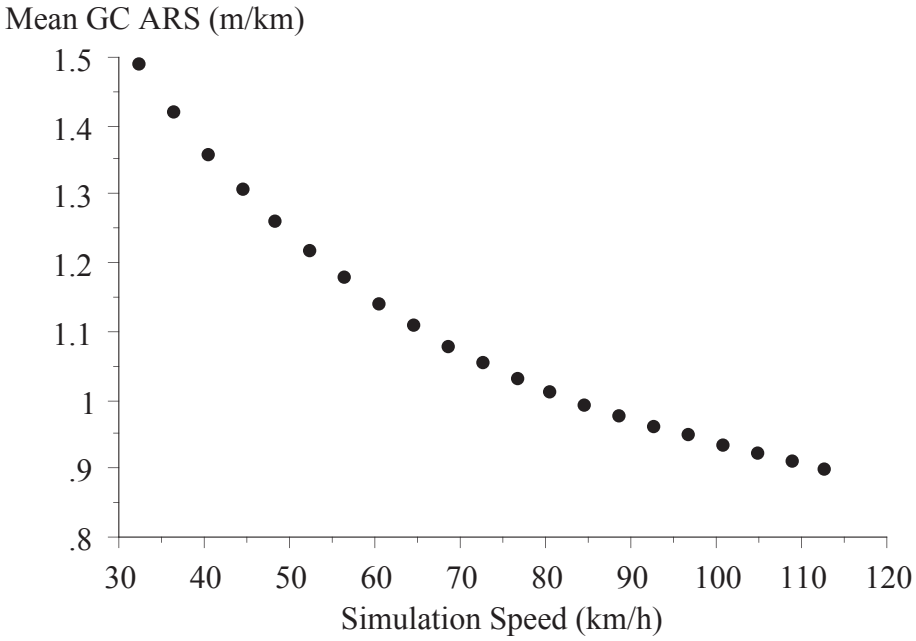

Figure 16. Effect of speed on a spatial Golden Car index, Section 32.

Note that the value decreases by nearly 40 percent as the speed increases from 32 km/h (20 mi/h) to 112 km/h (70 mi/h). The change occurs because as the speed increases, the sensitivity of the Golden Car model shifts toward longer wavelengths. (The same frequency corresponds to a proportionately longer wavelength at a higher speed.) The value of ARS decreases because the influence of the additional content that is "captured" at the long wavelength end is weaker than the content that is "left behind" at the short wavelength end. This is common among PCC pavements[32], where the content at the short wavelength end of the waveband affecting the IRI is often more significant than the content at the long wavelength end.[30] On Section 32, the changes with speed exhibited a very smooth, monotonically decreasing trend. On some of the test pavements from this study, this was not the case. On Section 21, for example, the content isolated at wavelengths of 2.0 m (6.4 ft) and 3.9 m (12.8 ft) interacted with the peak response of the Golden Car model at 9.66 Hz (2.30 m at 80 km/h) differently depending on simulation speed.

The trend in Figure 16 is seemingly at odds with the trends in vibration level observed on Section 32. Figure 17 shows that the measured point vibration total value at the floor/foot interface increased by nearly 80 percent over the same range of speeds. (This is not a direct comparison because the experimental test data cover 16 seconds of travel time, while the mean ARS values, above, are derived from profiles which all covered the entire length of pavement traversed in 16 seconds at 112 km/h.)

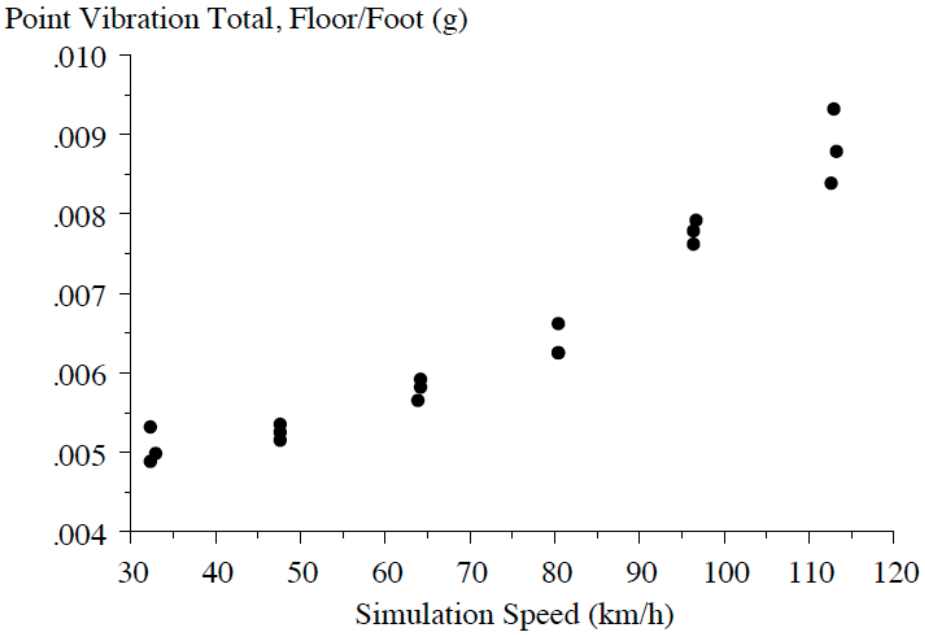

Figure 17. Effect of travel speed on measured vibration, Section 32.

The opposing trends show that the meaning of a "m/km" statistic depends heavily on the assumed travel speed. More predicted overall suspension motion occurs over the same travel distance at lower speed, even though the vibration level may be much less intense since it is spread out over a much longer time interval. Note that the absolute suspension stroke shown in Figure 16 is 65 percent higher at 32 km/h (20 mi/h) than it is at 112 km/h (70 mi/h), but it took place over a time that was 3.5 times greater. Had the intensity of vibration been represented as a function of time, rather than distance, the trend would reverse.

Figure 18 demonstrates this phenomenon, and shows the average rectified suspension stroking velocity (ARV) predicted by the Golden Car model as a function of speed. (This is obtained simply by multiplying the "m/km" by simulated travel speed in the appropriate units.) Here, the values increase aggressively with speed as the intensity of vibration within the Golden Car increases.

The "mean GC ARV" index shown in Figure 18 provides an assessment of the temporal intensity of the vibration. Thus, it may relate more closely to measured vibration. Figures 19 and 20 demonstrate the quality of this relationship for the midsize sedan and luxury SUV, respectively. In Figures 19 and 20, data from tests at target speeds from 96 km/h (60 mi/h) through 120 km/h (75 mi/h) all appear together, since the test speed and simulation speeds for each data pair match. For each value of OVT, the value

of mean GC ARV is simulated using the actual measured test speed for that run. When OVT is compared to mean GC ARV, a linear fit produces RMS residual values of 0.0059 g for the midsize sedan and 0.0052 g for the luxury SUV.

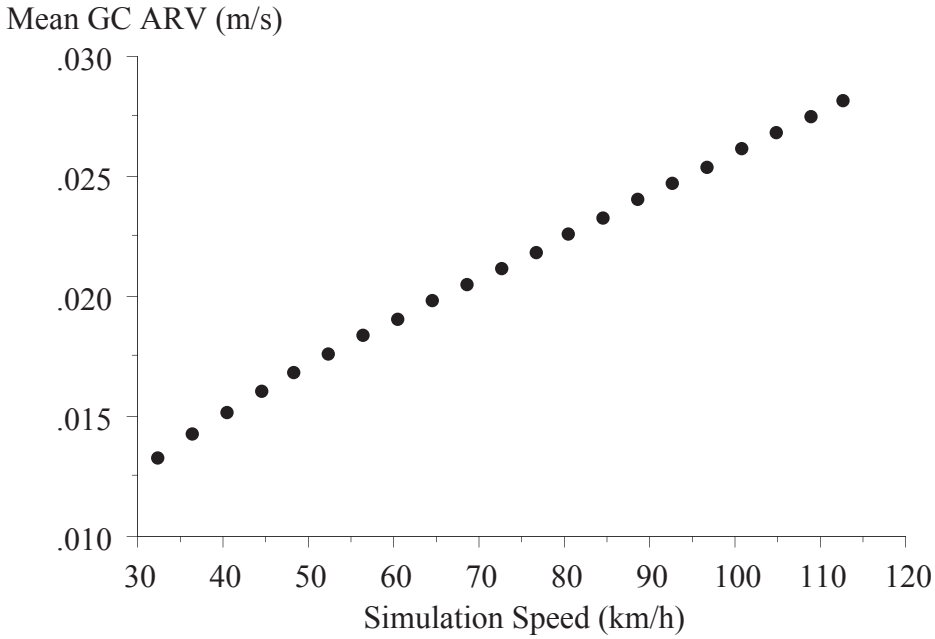

Figure 18. Effect of speed on a temporal Golden Car index, Section 32.

Mean GC ARV related to measured OVT no better than MRI for tests with target speeds of 96 km/h (60 mi/h) and 104 km/h (65 mi/h). Recall that the RMS residual values for a linear fit between OVT and MRI were 0.0055 g and 0.0053 g for the midsize sedan and luxury SUV, respectively. (See Figures 8 and 10.) On the other hand, mean GC ARV provided a significant improvement over MRI for tests performed with target speeds of 112 km/h (70 mi/h) and 120 km/h (75 mi/h). In this speed range, the RMS residual values were 0.0078 g and 0.0072 g for the midsize sedan and luxury SUV, respectively. The improvement is greater for tests at higher speeds since the measurements were performed at speeds with a much greater difference than the simulation speed used to calculate MRI.

Golden Car RMS Sprung Mass Acceleration

Figures 19 and 20 demonstrate the outcome of simulating the Golden Car at the actual test speed and using a temporal measure of road roughness. However, the mean GC ARV predicts the level of suspension stroke in an idealized vehicle, and this study examines measurements of acceleration. Using the Golden Car to predict RMS vertical acceleration at the sprung mass (i.e., the vehicle body) improves the linear relationship to OVT somewhat. Comparison of OVT to "mean GC ACC" index defined in the "Data Processing" section of this report reduced the RMS residual for a linear fit to 0.0046 g on both vehicles. (See Appendix B.) This index provides a single value for a lane by taking the average of the values from the left and right side.

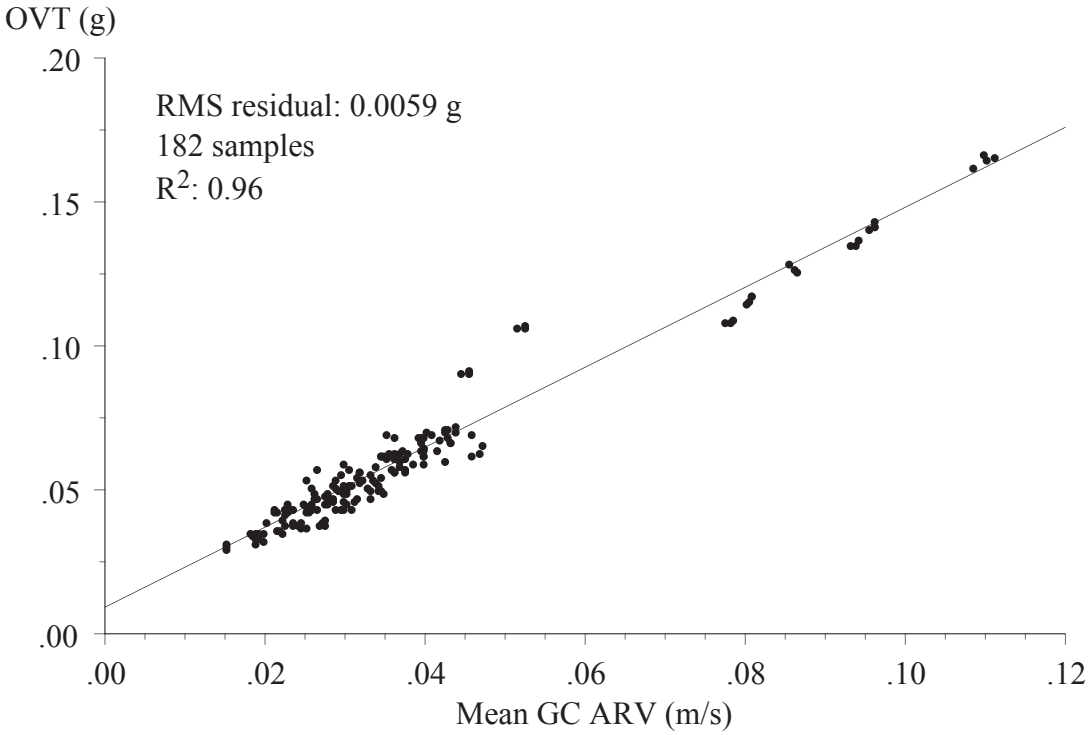

Figure 19. OVT versus mean GC ARV, midsize sedan, 96-120 km/h.

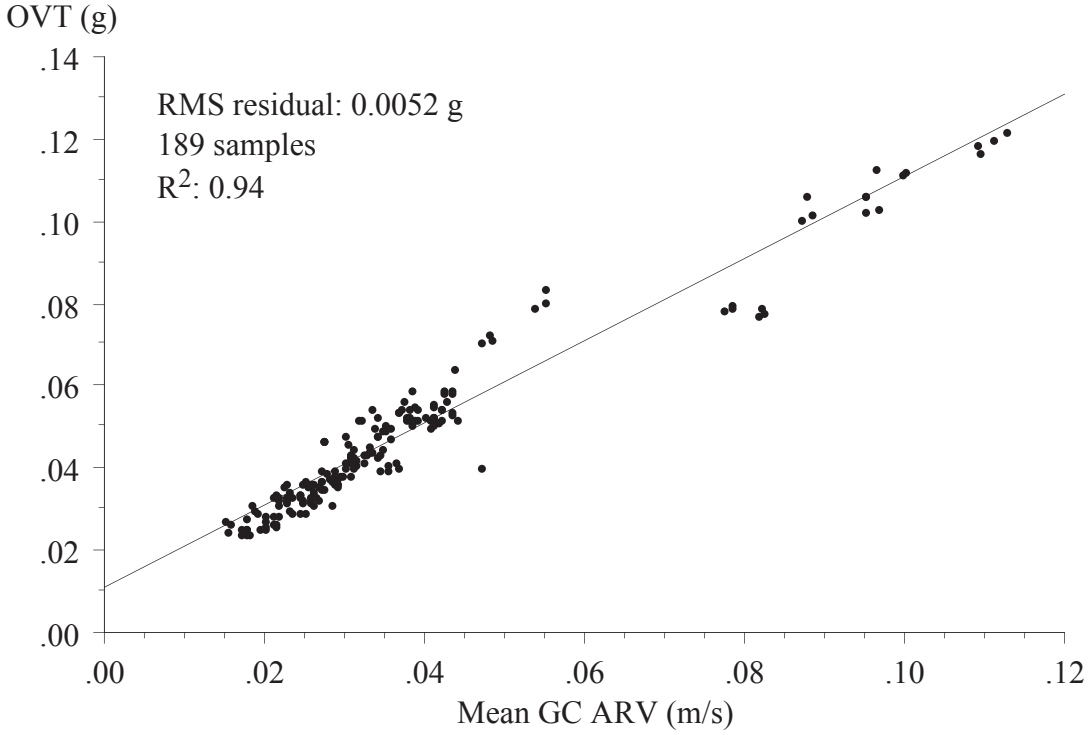

Figure 20. OVT versus mean GC ARV, luxury SUV, 96-120 km/h.

The OVT summarizes a combination of vibration levels in multiple directions and includes large contributions from responses at the seat. The Golden Car model, in contrast, predicts response in the vertical direction only without a model for seat/occupant dynamics or a provision for human comfort weighting functions. As such, the most appropriate quantity for comparison to sprung mass accelerations predicted by the Golden Car model may be vertical vibration at the floor/foot interface. Figure 21 illustrates this comparison for the luxury SUV. In this case, the quality of a linear fit is excellent, and the RMS residual is 0.0013 g. In contrast, the linear fit for the same comparison on the midsize sedan produced a RMS residual of 0.0058 g. This implies that the properties of the luxury SUV mixed with the influence of the frequency weighting function match the parameters of the Golden Car model more closely than the properties of the midsize sedan.

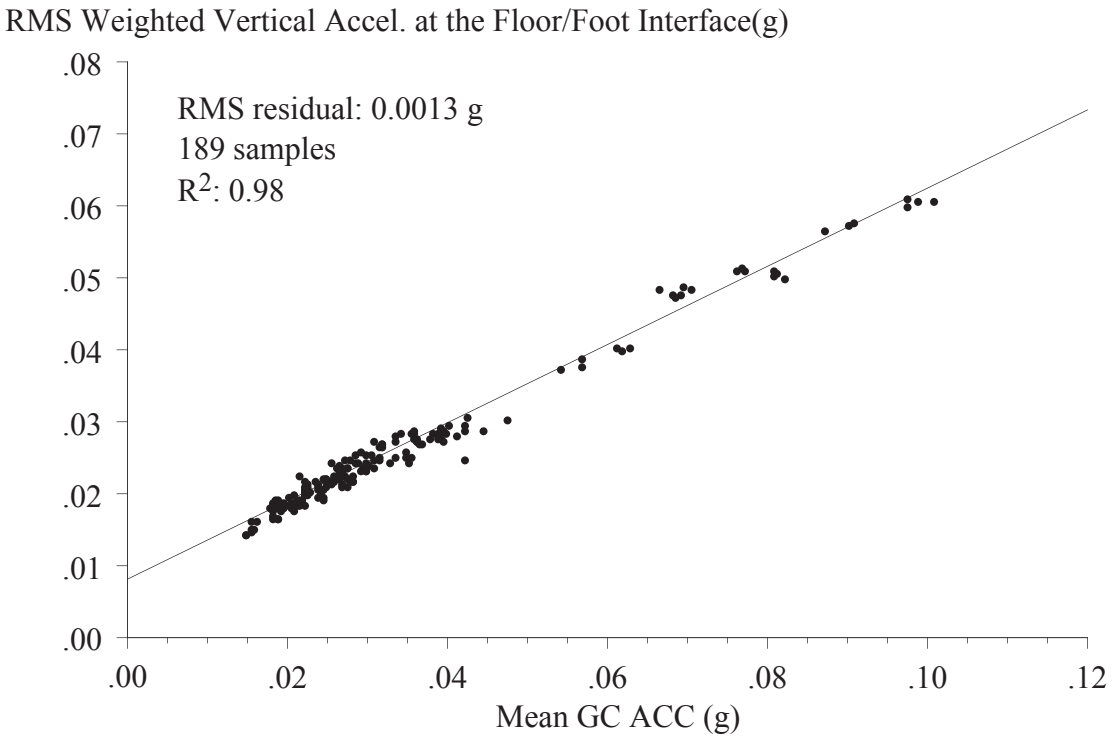

Figure 21. Vertical floor/foot vibration versus mean GC ACC, luxury SUV, 96-120 km/h.

Summary and Recommendations

This report examined the relationship between measurements of acceleration at vehicle/driver interfaces on smooth PCC pavements and the MRI from simultaneously measured longitudinal road profiles. The study included 32 test sections on freeways and state trunkline roads. Testing was performed with two instrumented vehicles: a midsize sedan and a luxury SUV. The measurements included accelerometers at three vehicle/driver interfaces: floor/foot, seat/buttock, and seat/back.

The experiment sought to determine if the IRI could indicate whether a PCC road provides acceptable ride quality for modern vehicles. For this study, the OVT defined by ISO 2631-1 provided an objective measure of the whole-body vibration level experienced by the driver over a given road segment. The OVT combined RMS vibration level from ten measured acceleration channels at three locations around the driver. The study also examined components of the OVT.

Overall, the MRI showed a close relationship to OVT on both test vehicles over a set of 30 PCC pavements. The statistical correlation was strong enough to justify smoothness specifications for ride quality based on the MRI, such that effort to minimize the MRI on PCC pavement provides a reasonable expectation that vibration level in passing road users would reduce commensurately. Data from the two AC sections tested in this study followed the relationship between OVT and MRI established on the PCC pavements. However, testing over broader conditions on AC may not follow the same trend.

The component of vibration that related to MRI best was vertical motion at the floor/foot interface. The excellent correlation between RMS acceleration there and MRI owes primarily to the fact the wavelength sensitivity to input profile of the computed MRI and measurements of weighted vertical acceleration at the floor/foot interface are similar. In contrast, the MRI displayed poor correlation to lateral acceleration in all three measurement locations. However, lateral vibration accounted for a small share of OVT in most of the tests (less than 5 percent in 342 of the 408 tests and less than 10 percent in 396 of the 408 tests).

Modifications to the MRI algorithm increased the level of correlation to OVT. In particular, measured vibration level changed significantly with speed, and custom indices based on the Golden Car model predicted OVT slightly better than MRI at very high travel speeds. Further improvements were observed when the Golden Car models produced a temporal index based on predicted acceleration in place of suspension stroke. However, since the MRI functions as a general pavement-surface condition indicator, it must maintain a standard definition and a reasonable level of relevance to a broad set of performance quantities (suspension stroke, tire loads, passenger acceleration) over a broad range of vehicle types and operating conditions (i.e., speeds). Seeking to optimize the MRI for one aspect of performance on a small set of test vehicles would compromise its broad relevance and overall value to pavement managers.

ISO 2631-1 provides ranges of OVT that correspond to verbal descriptions of "likely reactions" to seated passengers in public transport. Comparison of roughness levels to those ranges showed that:

- At highway speed, drivers will very rarely experience a level of whole-body vibration in the two test vehicles that is classified as "very uncomfortable" or "extremely uncomfortable" when the road has roughness deemed "acceptable" by the FHWA (this is, a road with MRI less than 2.68 m/km).
- For the two vehicles studied here, extra effort to reduce the MRI of a road below 0.5 m/km (31.6 in/mi) is not justified based on improvement in driver vibration level.

- Common ranges for full pay on new PCC surfaces in six states using the IRI for smoothness specifications overlap the "fairly uncomfortable" and "a little uncomfortable" ranges.

These results are encouraging, but the public's true reaction to road roughness depends heavily on their expectations and if the ride experience includes transient events (i.e., localized roughness).

Tire imbalance strongly affected the measured vibration level on the smoothest test sections, especially for vibration at the wheels and vibration experienced at the floor/foot interface. In some cases, as much as half of the RMS weighted lateral acceleration and a third of the RMS weighted vertical acceleration at the floor/foot interface could be traced to tire imbalance. With this in mind, unless extremely smooth pavement leads to a slower progression in roughness over time, decreasing roughness beneath the lowest levels covered in this study may not significantly improve the public's vibration experience.

These experiments provided some very useful context for MRI values on smooth PCC pavement. However, the measurements covered only a limited set of conditions, including a shallow speed range on most test sections, only two vehicles, and only 32 test sections. If the resources were available, measurements on a set of AC pavements, over a wider speed range, over more test sections with localized roughness, on more test vehicles, and throughout diurnal variations in curled PCC profiles would all provide significant additional value. A study of simulated vehicle response with a modest set of validation testing could provide much of this additional insight. As a minimum, commercial and custom multi-body codes exist that are well validated and could provide the breadth of conditions needed to define a limited, but informative testing program (i.e., use the simulations to test smart).

Simulation offers particular value in the study of vehicle behavior on very smooth pavement. For example, vehicle suspensions are much less effective on very smooth roads. This is because a minimal level of dynamic activity is needed to overcome the friction in suspension components. Further, the influence of other sources of vibration in a vehicle besides road roughness, such as tire imbalance, wind, and engine vibration, may be quantified in the absence of measurement system noise.

This study attempted to establish a link between reducing MRI and improvement in ride quality on PCC pavement. While ride quality is a very important functional outcome of a road's longitudinal profile, similar information on the incremental value of reducing roughness is also needed for the dynamic component of truck loading on pavements, vehicle wear, and energy losses at the tires and suspensions.

References

1. ISO 2631-1: 1997. Mechanical Vibration and Shock. Evaluation of Human Exposure to Whole-body Vibration.
2. Sayers, M. W., "On the Calculation of International Roughness Index from Longitudinal Road Profile." *Transportation Research Record 1501* (1995) pp. 1-12.

3. Gordon, T. J. and Z. Bareket, "Vibration Transmission from Road Surface Features - Measurement and Detection." *University of Michigan Transportation Research Institute Report UMTRI-2007-4* (2007) 50 p.
4. LeBlanc, D., et al., "Road Departure Crash Warning System Field Operational Test: Methodology and Results." *University of Michigan Transportation Research Institute Report UMTRI-2006-9-1* (2006) 307 p.
5. SAE J670f: (2007) Vehicle Dynamics Terminology.
6. Karamihas, S. M. and T. D. Gillespie, "Assessment of Profiler Performance for Construction Quality Control: Phase I." Portland Cement Association, *PCA R&D Serial No. 2887* (2005) 22 p.
7. Karamihas, S. M., "2005 ACPA Profiler Repeatability Tests." *University of Michigan Transportation Research Institute Report UMTRI-2005-35* (2005) 24 p.
8. "Weight, Height, and Selected Body Dimensions of Adults. United States 1960-1962." U.S. Department of Health, Education, and Welfare Publication No. (HRA) 76-1074.
9. "Height and Weight of Adults Ages 18-74 Years by Socioeconomic and Geographic Variables. United States." U.S. Department of Health and Human Services Publication No. (PHS) 81-2674.
10. "Weight and Height of Adults 18-74 Years of Age: United States, 1971-1974." U.S. Department of Health, Education, and Welfare Publication No. (PHS) 79-1659.
11. European Bus Directive 2001/85/EC, part 7.4.2.1.
12. Spangler, E. B. and Kelley, W. J., "GMR Road Profilometer–A Method for Measuring Road Profile," General Motor Research Laboratory, Warren Michigan, *Research Publication GMR-452* (1964) 44 p.
13. Butkunas, A.A., "Power Spectral Density and Ride Evaluation." *Society of Automotive Engineers Paper No. 660138* (1966).
14. Griffin, M. J., "Evaluation of Vibration with Respect to Human Response." *Society of Automotive Engineers P-174* (1986) pp. 11-34.
15. Donati, P., et al., "The Subjective Equivalence of Sinusoidal and Random Whole-Body Vibration in a Sitting Position (an Experimental Study Using the Floating Reference Vibration Method)." *Ergonomics*, Vol. 26, No. 3 (1983) pp. 251-273.
16. Fothergill, L. C. and M. J. Griffin, "The Evaluation of Discomfort Produced by Multiple Frequency Whole-Body Vibration." *Ergonomics*, Vol. 20, No. 3 (1977) pp. 263-276.
17. Griffin, M. J., Parsons, K. C., and E. M. Whitham, "Vibration and Comfort. I:Translational Seat Vibration." *Ergonomics*, Vol. 25, No. 7 (1982) pp. 603-630.

18. Jones, A. J., and D. J. Saunders, "Equal Comfort Contours for Whole Body Vertical, Pulsed Sinusoidal Vibration." *Journal of Sound and Vibration*, Vol. 23, No. 1 (1972) pp. 1-14.

19. Lee, R. A. and F. Pradko, "Analytical Analysis of Human Vibration." *Society of Automotive Engineers Paper No. 680091* (1968) 14 p.

20. Miwa, T., "Evaluation Methods for Vibration Effect: Part 1 Measurements of Threshold and Equal Sensation Contours of Whole Body Vertical and Horizontal Vibration." *Industrial Health*, Vol. 5 (1967) pp. 183-205.

21. Parsons, K. C. and M. J. Griffin, "Vibration and Comfort. II Rotational Seat Vibration." *Ergonomics*, Vo. 25, No. 7 (1982) pp. 631-644.

22. Sayers, M. W. and S. M. Karamihas, *The Little Book of Profiling.* University of Michigan Transportation Research Institute (1998) 100 p.

23. Sayers, M. W., et al., "Guidelines for Conducting and Calibrating Road Roughness Measurements." *World Bank Technical Paper Number 46* (1986) 87 p.

24. Sayers, M. W., "On the Calculation of International Roughness Index from Longitudinal Road Profile." *Transportation Research Record 1501* (1995) pp 1-12.

25. Sayers, M. W., et al., "The International Road Roughness Experiment." *World Bank Technical Paper Number 45* (1986) 453 p.

26. Karamihas, S. M. et al., "Guidelines for Longitudinal Pavement Profile Measurement." *National Cooperative Highway Research Program Report 434* (2000) 75 p.

27. Sayers, M. W., "Two Quarter-Car Models for Defining Road Roughness: IRI and HRI." *Transportation Research Record 1215* (1989) pp. 165-172.

28. Gillespie, T. D., et al., "Calibration of Response-Type Road Roughness Measuring Systems." *National Cooperative Highway Research Program Report 228* (1980) 81 p.

29. Karamihas, S. M., Gillespie, T. D. and S. M. Riley, "Axle Tramp Contribution to the Dynamic Wheel Loads of a Heavy Truck." *Proceedings of the Fourth International Symposium on Heavy Vehicle Weights and Dimensions*, Ann Arbor, Michigan. Ed. C. B. Winkler. (1995) pp. 425-434.

30. Sayers, M. W., "Characteristic Power Spectral Density Functions for Vertical and Roll Components of Road Roughness." American Society of Mechanical Engineers. *AMD-Vol. 80*. (1986) pp. 113-129.

31. Wilde, W. J., "Implementation of an International Roughness Index for Mn/DOT Pavement Condition and Rehabilitation." *Minnesota Department of Transportation Report MN/RC-2007-09* (2007) 133 p.

32. Perera, R. W. and S. D. Kohn, "Effects of Variation in Quarter-Car Simulation Speed on International Roughness Index Algorithm." *Transportation Research Record 1889* (2004) pp. 144-151.

Appendix A: Valid Run Counts

After data quality checks, the data in this study included 408 valid test runs. For each combination of test section, test vehicle, and target speed, at least three, and in some cases four, valid runs were collected. Tables A-1 and A-2 list the number of runs considered in this study by test section and target speed for each vehicle.

Table A-1. Valid runs by vehicle and target speed, midsize sedan.

Section	Target Speed (km/h)	Average Speed (km/h)	Valid Runs	Target Speed (km/h)	Average Speed (km/h)	Valid Runs
01	104	104.0	3	120	119.7	3
02	96	96.0	3	112	112.7	3
03	104	104.4	3	120	119.3	3
04	96	94.9	3	112	111.1	3
05	104	102.0	3	120	117.4	3
06	104	103.3	3	120	119.7	3
07	104	103.2	3	120	118.5	3
08	104	104.4	4	120	119.5	3
09	96	94.8	3	112	110.8	3
10	96	93.8	3	112	109.8	3
11	104	103.5	3	120	120.2	3
12	104	103.6	3	120	119.3	3
13	104	103.3	4	120	119.3	3
14	104	102.2	3	120	118.3	3
15	96	94.8	3	112	110.7	4
16	96	96.0	3	112	111.4	3
17	96	96.2	4	112	111.3	3
18	96	95.6	3	112	110.9	3
19	104	102.5	3	120	117.9	3
20	96	94.7	3	112	110.7	3
21	104	101.9	3	120	117.7	3
22	104	103.2	3	120	120.0	3
23	104	103.9	3	120	119.2	3
24	104	101.7	3	120	117.6	3
25	96	95.9	3	112	111.6	3
26	96	95.5	4	112	111.2	4
27	96	95.2	3	112	111.2	4
28	96	95.9	3	112	111.9	3
29	104	104.3	4	120	119.7	3
30	96	95.9	4	112	111.8	3
31	104	104.3	3	120	119.6	3

Table A-2. Valid runs by vehicle and target speed, luxury SUV.

Section	Target Speed (km/h)	Average Speed (km/h)	Valid Runs	Target Speed (km/h)	Average Speed (km/h)	Valid Runs
01	104	103.7	3	120	119.8	3
02	96	96.1	4	112	111.8	3
03	104	104.6	3	120	120.7	3
04	96	95.1	3	112	111.1	3
05	104	101.8	3	120	117.7	3
06	104	104.0	3	120	119.6	3
07	104	103.5	4	120	119.2	3
08	104	104.4	3	120	119.3	3
09	96	94.6	3	112	110.5	3
10	96	93.6	3	112	109.3	3
11	104	103.4	3	120	119.6	3
12	104	103.4	3	120	119.3	3
13	104	103.5	3	120	119.6	3
14	104	102.4	3	120	118.3	3
15	96	95.0	3	112	110.9	3
16	96	95.8	3	112	111.5	3
17	96	95.9	4	112	112.5	3
18	96	96.0	3	112	110.9	3
19	104	102.2	4	120	118.2	4
20	96	94.9	3	112	110.8	3
21	104	102.3	3	120	118.0	4
22	104	103.7	3	120	118.6	3
23	104	103.8	3	120	119.7	3
24	104	102.3	3	120	118.2	3
25	96	95.6	3	112	111.6	4
26	96	95.7	3	112	111.2	4
27	96	95.3	3	112	111.3	3
28	96	96.4	3	112	112.1	3
29	104	103.5	3	120	119.5	3
30	96	95.8	3	112	112.1	3
31	104	104.4	4	120	120.1	3
32	96	96.3	3	112	112.8	3
32	64	63.9	3	80	80.3	3
32	32	32.4	3	48	47.4	3

Appendix B: Regression Statistics

This appendix provides regression statistics and plots not included in the main report. All of the plots and statistics pertain to a linear fit between a ride vibration summary statistic for the entire 16-second ride experience and a roughness index for the entire length of pavement covered in that time.

The ride statistics include: the overall vibration total value (OVT), a point vibration total at the floor/foot interface (PVT Floor/Foot), a point vibration total at the seat/buttock interface (PVT Seat/Butt), a point vibration total at the seat/back interface (PVT Seat/Back), the RMS vertical vibration at the seat/buttock interface (Seat/Butt Z), and the RMS vertical vibration at the floor/foot interface (Floor/Foot Z).

The conventional roughness statistics include four standard indices derived from the IRI: MRI, HRI, left IRI, right IRI. The roughness statistics also include:

- Golden Car Average Rectified Suspension Stroking Velocity (GC ARV): This index is calculated by simulating the Golden Car model at the actual test speed, and accumulating the average rectified suspension stroking velocity over a given interval. The index from the left side only, the right side only, and the average of the left and right were calculated.
- RMS Golden Car Spring Mass Acceleration (GC ACC): This index provides the RMS value of vertical acceleration of the sprung mass predicted by the Golden Car model at the actual test speed.

This appendix examined individual values from each of the left and right profiles, as well as a dual wheel track version of each index. For GC ARV and GC ACC, the dual wheel track value was the average of the index from the left and right side.

Table B-1 lists regression statistics for vibration summary statistics versus roughness index on all tests performed on PCC pavement at target speeds from 96 km/h (60 mi/h) to 120 km/h (75 mi/h). Table B-2 covers all tests performed on any pavement at target speeds from 96 km/h (60 mi/h) to 120 km/h (75 mi/h). As such, the data in Table B-2 includes tests on two AC pavement sections with MRI values of 0.48 m/km (31 in/mi) and 0.58 m/km (37 in/mi). Figures B-1 through B-10 provide scatter plots that match Figures 8 through 11 and 19 through 21 from the main report, with data from the two AC sections added.

Table B-1. Regression statistics, PCC sections only.

Vehicle	Speed Range (km/h)	Roughness Index	Vibration Value	Samples	RMS Residual (g x10^{-4})	R^2
midsize sedan	96-104	MRI	OVT	92	55	0.96
			PVT Floor/Foot	92	13	0.97
			PVT Seat/Butt	92	55	0.95
			PVT Seat/Back	92	19	0.93
			Seat/Butt Z	92	22	0.96
			Floor/Foot Z	92	34	0.97
		HRI	OVT	92	59	0.95
			PVT Floor/Foot	92	13	0.97
			PVT Seat/Butt	92	58	0.95
			PVT Seat/Back	92	19	0.92
			Seat/Butt Z	92	22	0.95
			Floor/Foot Z	92	35	0.97
		Left IRI	OVT	92	61	0.95
			PVT Floor/Foot	92	16	0.95
			PVT Seat/Butt	92	59	0.95
			PVT Seat/Back	92	19	0.92
			Seat/Butt Z	92	26	0.94
			Floor/Foot Z	92	42	0.95
		Right IRI	OVT	92	62	0.95
			PVT Floor/Foot	92	14	0.96
			PVT Seat/Butt	92	61	0.94
			PVT Seat/Back	92	20	0.91
			Seat/Butt Z	92	22	0.95
			Floor/Foot Z	92	37	0.96
	112-120	MRI	OVT	90	78	0.94
			PVT Floor/Foot	90	14	0.97
			PVT Seat/Butt	90	76	0.93
			PVT Seat/Back	90	27	0.89
			Seat/Butt Z	90	32	0.94
			Floor/Foot Z	90	37	0.97
		HRI	OVT	90	80	0.93
			PVT Floor/Foot	90	14	0.97
			PVT Seat/Butt	90	78	0.93
			PVT Seat/Back	90	27	0.88
			Seat/Butt Z	90	32	0.94
			Floor/Foot Z	90	39	0.97
		Left IRI	OVT	90	84	0.93
			PVT Floor/Foot	90	15	0.97
			PVT Seat/Butt	90	81	0.92
			PVT Seat/Back	90	28	0.88
			Seat/Butt Z	90	33	0.93
			Floor/Foot Z	90	41	0.96
		Right IRI	OVT	90	82	0.93
			PVT Floor/Foot	90	17	0.96
			PVT Seat/Butt	90	80	0.93
			PVT Seat/Back	90	27	0.88
			Seat/Butt Z	90	34	0.93
			Floor/Foot Z	90	44	0.96

Table B-1 (cont.). Regression statistics, PCC sections only.

Vehicle	Speed Range (km/h)	Roughness Index	Vibration Value	Samples	RMS Residual (g x10^{-4})	R^2
luxury SUV	96-104	MRI	OVT	95	53	0.93
			PVT Floor/Foot	95	7	0.97
			PVT Seat/Butt	95	51	0.93
			PVT Seat/Back	95	20	0.92
			Seat/Butt Z	95	17	0.95
			Floor/Foot Z	95	17	0.97
		HRI	OVT	95	56	0.93
			PVT Floor/Foot	95	8	0.96
			PVT Seat/Butt	95	53	0.92
			PVT Seat/Back	95	21	0.91
			Seat/Butt Z	95	18	0.94
			Floor/Foot Z	95	19	0.96
		Left IRI	OVT	95	53	0.93
			PVT Floor/Foot	95	7	0.97
			PVT Seat/Butt	95	51	0.93
			PVT Seat/Back	95	20	0.92
			Seat/Butt Z	95	16	0.95
			Floor/Foot Z	95	17	0.97
		Right IRI	OVT	95	57	0.92
			PVT Floor/Foot	95	8	0.96
			PVT Seat/Butt	95	54	0.92
			PVT Seat/Back	95	21	0.90
			Seat/Butt Z	95	19	0.93
			Floor/Foot Z	95	21	0.96
	112-120	MRI	OVT	94	72	0.90
			PVT Floor/Foot	94	8	0.97
			PVT Seat/Butt	94	69	0.90
			PVT Seat/Back	94	27	0.88
			Seat/Butt Z	94	27	0.90
			Floor/Foot Z	94	20	0.97
		HRI	OVT	94	73	0.90
			PVT Floor/Foot	94	9	0.96
			PVT Seat/Butt	94	70	0.89
			PVT Seat/Back	94	27	0.88
			Seat/Butt Z	94	28	0.89
			Floor/Foot Z	94	21	0.96
		Left IRI	OVT	94	71	0.90
			PVT Floor/Foot	94	8	0.97
			PVT Seat/Butt	94	68	0.90
			PVT Seat/Back	94	26	0.88
			Seat/Butt Z	94	26	0.90
			Floor/Foot Z	94	20	0.97
		Right IRI	OVT	94	77	0.89
			PVT Floor/Foot	94	10	0.95
			PVT Seat/Butt	94	73	0.88
			PVT Seat/Back	94	28	0.87
			Seat/Butt Z	94	29	0.88
			Floor/Foot Z	94	23	0.95

Table B-1 (cont.). Regression statistics, PCC sections only.

Vehicle	Speed Range (km/h)	Roughness Index	Vibration Value	Samples	RMS Residual (g x10^{-4})	R^2
midsize sedan	96-120	Mean GC ARV	OVT	182	59	0.96
			PVT Floor/Foot	182	17	0.95
			PVT Seat/Butt	182	58	0.96
			PVT Seat/Back	182	20	0.93
			Seat/Butt Z	182	28	0.94
			Floor/Foot Z	182	44	0.95
		Left GC ARV	OVT	182	66	0.95
			PVT Floor/Foot	182	19	0.94
			PVT Seat/Butt	182	65	0.95
			PVT Seat/Back	182	20	0.93
			Seat/Butt Z	182	29	0.94
			Floor/Foot Z	182	50	0.94
		Right GC ARV	OVT	182	63	0.95
			PVT Floor/Foot	182	18	0.95
			PVT Seat/Butt	182	62	0.95
			PVT Seat/Back	182	21	0.92
			Seat/Butt Z	182	30	0.93
			Floor/Foot Z	182	46	0.95
luxury SUV	96-120	Mean GC ARV	OVT	189	52	0.94
			PVT Floor/Foot	189	7	0.97
			PVT Seat/Butt	189	50	0.94
			PVT Seat/Back	189	20	0.92
			Seat/Butt Z	189	19	0.94
			Floor/Foot Z	189	18	0.97
		Left GC ARV	OVT	189	53	0.94
			PVT Floor/Foot	189	8	0.97
			PVT Seat/Butt	189	50	0.94
			PVT Seat/Back	189	20	0.92
			Seat/Butt Z	189	18	0.95
			Floor/Foot Z	189	19	0.97
		Right GC ARV	OVT	189	57	0.93
			PVT Floor/Foot	189	8	0.96
			PVT Seat/Butt	189	55	0.93
			PVT Seat/Back	189	21	0.91
			Seat/Butt Z	189	21	0.93
			Floor/Foot Z	189	20	0.96

Table B-1 (cont.). Regression statistics, PCC sections only.

Vehicle	Speed Range (km/h)	Roughness Index	Vibration Value	Samples	RMS Residual (g x10^{-4})	R^2
midsize sedan	96-120	Mean GC ACC	OVT	182	46	0.98
			PVT Floor/Foot	182	23	0.92
			PVT Seat/Butt	182	44	0.98
			PVT Seat/Back	182	14	0.96
			Seat/Butt Z	182	36	0.91
			Floor/Foot Z	182	58	0.91
		Left GC ACC	OVT	182	63	0.96
			PVT Floor/Foot	182	26	0.90
			PVT Seat/Butt	182	60	0.95
			PVT Seat/Back	182	17	0.95
			Seat/Butt Z	182	38	0.89
			Floor/Foot Z	182	65	0.89
		Right GC ACC	OVT	182	50	0.97
			PVT Floor/Foot	182	23	0.91
			PVT Seat/Butt	182	47	0.97
			PVT Seat/Back	182	16	0.95
			Seat/Butt Z	182	37	0.90
			Floor/Foot Z	182	59	0.91
luxury SUV	96-120	Mean GC ACC	OVT	189	46	0.96
			PVT Floor/Foot	189	6	0.98
			PVT Seat/Butt	189	46	0.95
			PVT Seat/Back	189	15	0.96
			Seat/Butt Z	189	14	0.97
			Floor/Foot Z	189	13	0.98
		Left GC ACC	OVT	189	48	0.95
			PVT Floor/Foot	189	7	0.98
			PVT Seat/Butt	189	48	0.94
			PVT Seat/Back	189	16	0.95
			Seat/Butt Z	189	14	0.97
			Floor/Foot Z	189	16	0.98
		Right GC ACC	OVT	189	52	0.94
			PVT Floor/Foot	189	7	0.97
			PVT Seat/Butt	189	51	0.94
			PVT Seat/Back	189	17	0.95
			Seat/Butt Z	189	17	0.95
			Floor/Foot Z	189	18	0.97

Table B-2. Regression statistics, all test sections.

Vehicle	Speed Range (km/h)	Roughness Index	Vibration Value	Samples	RMS Residual (g x10^{-4})	R^2
midsize sedan	96-104	MRI	OVT	99	54	0.96
			PVT Floor/Foot	99	13	0.97
			PVT Seat/Butt	99	53	0.96
			PVT Seat/Back	99	18	0.93
			Seat/Butt Z	99	22	0.96
			Floor/Foot Z	99	33	0.97
		HRI	OVT	99	57	0.96
			PVT Floor/Foot	99	13	0.97
			PVT Seat/Butt	99	56	0.95
			PVT Seat/Back	99	19	0.92
			Seat/Butt Z	99	22	0.96
			Floor/Foot Z	99	34	0.97
		Left IRI	OVT	99	60	0.95
			PVT Floor/Foot	99	16	0.96
			PVT Seat/Butt	99	58	0.95
			PVT Seat/Back	99	19	0.92
			Seat/Butt Z	99	25	0.94
			Floor/Foot Z	99	41	0.95
		Right IRI	OVT	99	60	0.95
			PVT Floor/Foot	99	14	0.97
			PVT Seat/Butt	99	59	0.95
			PVT Seat/Back	99	20	0.92
			Seat/Butt Z	99	22	0.95
			Floor/Foot Z	99	36	0.96
	112-120	MRI	OVT	96	77	0.94
			PVT Floor/Foot	96	14	0.97
			PVT Seat/Butt	96	75	0.94
			PVT Seat/Back	96	26	0.89
			Seat/Butt Z	96	31	0.94
			Floor/Foot Z	96	36	0.97
		HRI	OVT	96	79	0.94
			PVT Floor/Foot	96	14	0.97
			PVT Seat/Butt	96	77	0.93
			PVT Seat/Back	96	27	0.88
			Seat/Butt Z	96	31	0.94
			Floor/Foot Z	96	37	0.97
		Left IRI	OVT	96	84	0.93
			PVT Floor/Foot	96	16	0.97
			PVT Seat/Butt	96	81	0.92
			PVT Seat/Back	96	28	0.87
			Seat/Butt Z	96	33	0.94
			Floor/Foot Z	96	41	0.96
		Right IRI	OVT	96	80	0.94
			PVT Floor/Foot	96	17	0.96
			PVT Seat/Butt	96	78	0.93
			PVT Seat/Back	96	27	0.88
			Seat/Butt Z	96	34	0.93
			Floor/Foot Z	96	42	0.96

Table B-2 (cont.). Regression statistics, all test sections.

Vehicle	Speed Range (km/h)	Roughness Index	Vibration Value	Samples	RMS Residual (g x10^{-4})	R^2
luxury SUV	96-104	MRI	OVT	101	52	0.94
			PVT Floor/Foot	101	7	0.97
			PVT Seat/Butt	101	49	0.93
			PVT Seat/Back	101	20	0.91
			Seat/Butt Z	101	17	0.95
			Floor/Foot Z	101	17	0.97
		HRI	OVT	101	54	0.93
			PVT Floor/Foot	101	8	0.96
			PVT Seat/Butt	101	51	0.93
			PVT Seat/Back	101	20	0.91
			Seat/Butt Z	101	18	0.94
			Floor/Foot Z	101	19	0.96
		Left IRI	OVT	101	53	0.93
			PVT Floor/Foot	101	7	0.97
			PVT Seat/Butt	101	50	0.93
			PVT Seat/Back	101	20	0.91
			Seat/Butt Z	101	16	0.95
			Floor/Foot Z	101	17	0.97
		Right IRI	OVT	101	55	0.93
			PVT Floor/Foot	101	8	0.96
			PVT Seat/Butt	101	52	0.92
			PVT Seat/Back	101	21	0.91
			Seat/Butt Z	101	18	0.94
			Floor/Foot Z	101	20	0.96
	112-120	MRI	OVT	100	71	0.90
			PVT Floor/Foot	100	8	0.96
			PVT Seat/Butt	100	67	0.90
			PVT Seat/Back	100	27	0.88
			Seat/Butt Z	100	27	0.90
			Floor/Foot Z	100	20	0.97
		HRI	OVT	100	72	0.90
			PVT Floor/Foot	100	9	0.96
			PVT Seat/Butt	100	68	0.90
			PVT Seat/Back	100	27	0.87
			Seat/Butt Z	100	27	0.89
			Floor/Foot Z	100	21	0.96
		Left IRI	OVT	100	71	0.90
			PVT Floor/Foot	100	8	0.96
			PVT Seat/Butt	100	67	0.90
			PVT Seat/Back	100	27	0.90
			Seat/Butt Z	100	27	0.90
			Floor/Foot Z	100	20	0.96
		Right IRI	OVT	100	75	0.89
			PVT Floor/Foot	100	9	0.95
			PVT Seat/Butt	100	71	0.89
			PVT Seat/Back	100	28	0.86
			Seat/Butt Z	100	29	0.88
			Floor/Foot Z	100	23	0.95

Table B-2 (cont.). Regression statistics, all test sections.

Vehicle	Speed Range (km/h)	Roughness Index	Vibration Value	Samples	RMS Residual (g x10^{-4})	R^2
midsize sedan	96-120	Mean GC ARV	OVT	195	58	0.96
			PVT Floor/Foot	195	17	0.96
			PVT Seat/Butt	195	57	0.96
			PVT Seat/Back	195	19	0.93
			Seat/Butt Z	195	27	0.95
			Floor/Foot Z	195	43	0.95
		Left GC ARV	OVT	195	66	0.95
			PVT Floor/Foot	195	19	0.94
			PVT Seat/Butt	195	64	0.95
			PVT Seat/Back	195	20	0.92
			Seat/Butt Z	195	28	0.94
			Floor/Foot Z	195	48	0.94
		Right GC ARV	OVT	195	62	0.96
			PVT Floor/Foot	195	17	0.95
			PVT Seat/Butt	195	60	0.95
			PVT Seat/Back	195	21	0.92
			Seat/Butt Z	195	29	0.94
			Floor/Foot Z	195	44	0.95
luxury SUV	96-120	Mean GC ARV	OVT	201	51	0.94
			PVT Floor/Foot	201	7	0.97
			PVT Seat/Butt	201	49	0.94
			PVT Seat/Back	201	20	0.92
			Seat/Butt Z	201	19	0.94
			Floor/Foot Z	201	17	0.97
		Left GC ARV	OVT	201	52	0.94
			PVT Floor/Foot	201	8	0.97
			PVT Seat/Butt	201	50	0.94
			PVT Seat/Back	201	21	0.92
			Seat/Butt Z	201	19	0.95
			Floor/Foot Z	201	19	0.97
		Right GC ARV	OVT	201	56	0.93
			PVT Floor/Foot	201	8	0.96
			PVT Seat/Butt	201	53	0.93
			PVT Seat/Back	201	21	0.91
			Seat/Butt Z	201	21	0.93
			Floor/Foot Z	201	19	0.97

Table B-2 (cont.). Regression statistics, all test sections.

Vehicle	Speed Range (km/h)	Roughness Index	Vibration Value	Samples	RMS Residual (g x10^{-4})	R^2
midsize sedan	96-120	Mean GC ACC	OVT	195	44	0.98
			PVT Floor/Foot	195	22	0.92
			PVT Seat/Butt	195	42	0.98
			PVT Seat/Back	195	14	0.96
			Seat/Butt Z	195	36	0.91
			Floor/Foot Z	195	58	0.92
		Left GC ACC	OVT	195	61	0.96
			PVT Floor/Foot	195	25	0.90
			PVT Seat/Butt	195	58	0.96
			PVT Seat/Back	195	17	0.95
			Seat/Butt Z	195	38	0.90
			Floor/Foot Z	195	64	0.90
		Right GC ACC	OVT	195	50	0.97
			PVT Floor/Foot	195	23	0.92
			PVT Seat/Butt	195	47	0.97
			PVT Seat/Back	195	16	0.95
			Seat/Butt Z	195	38	0.90
			Floor/Foot Z	195	59	0.91
luxury SUV	96-120	Mean GC ACC	OVT	201	44	0.96
			PVT Floor/Foot	201	5	0.98
			PVT Seat/Butt	201	44	0.95
			PVT Seat/Back	201	14	0.96
			Seat/Butt Z	201	13	0.97
			Floor/Foot Z	201	13	0.98
		Left GC ACC	OVT	201	47	0.95
			PVT Floor/Foot	201	6	0.98
			PVT Seat/Butt	201	47	0.95
			PVT Seat/Back	201	15	0.96
			Seat/Butt Z	201	13	0.97
			Floor/Foot Z	201	16	0.98
		Right GC ACC	OVT	201	51	0.95
			PVT Floor/Foot	201	7	0.97
			PVT Seat/Butt	201	50	0.94
			PVT Seat/Back	201	17	0.95
			Seat/Butt Z	201	17	0.95
			Floor/Foot Z	201	17	0.97

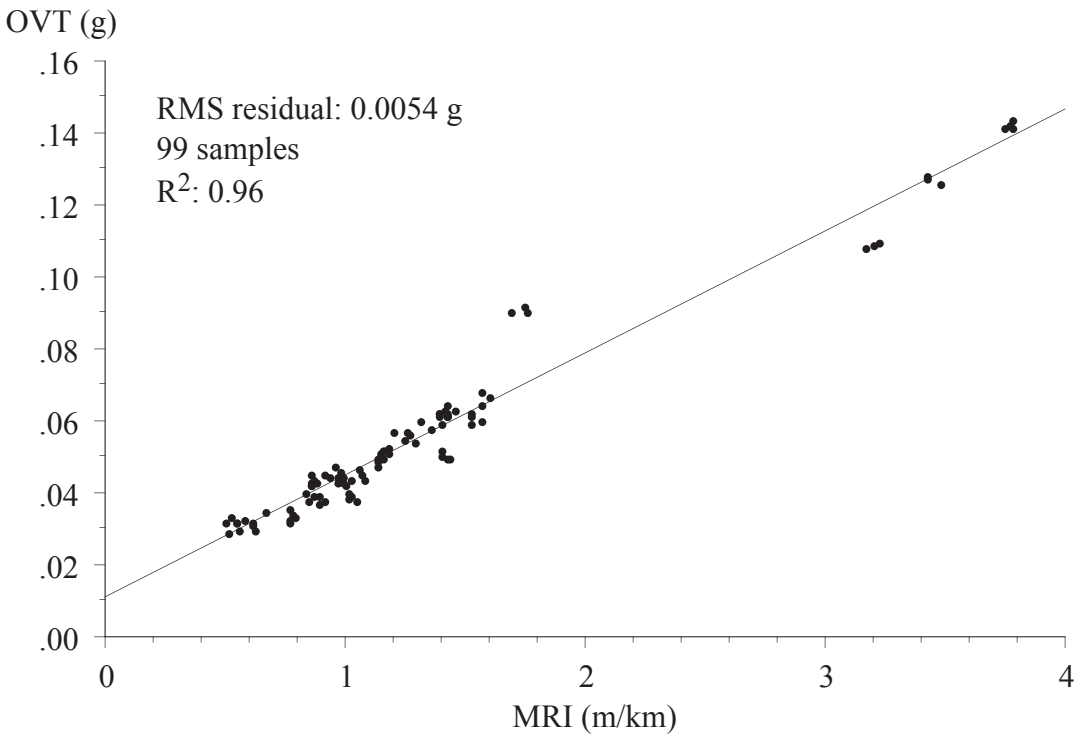

Figure B-1. OVT versus MRI, midsize sedan, 96-104 km/h.

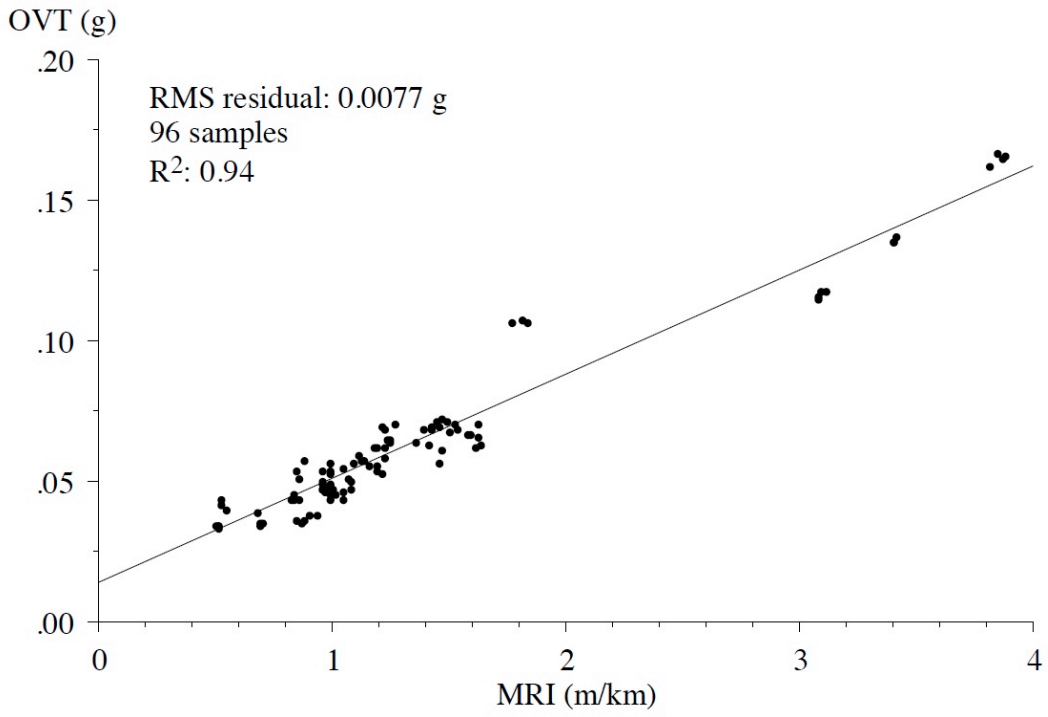

Figure B-2. OVT versus MRI, midsize sedan, 112-120 km/h.

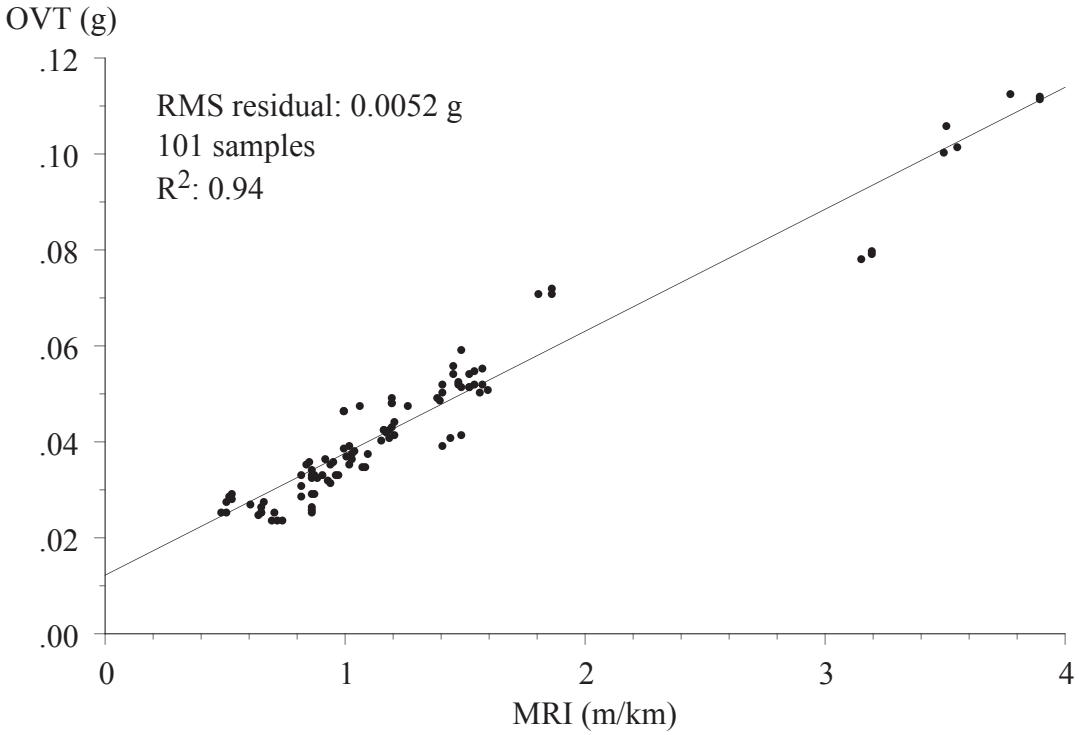

Figure B-3. OVT versus MRI, luxury SUV, 96-104 km/h.

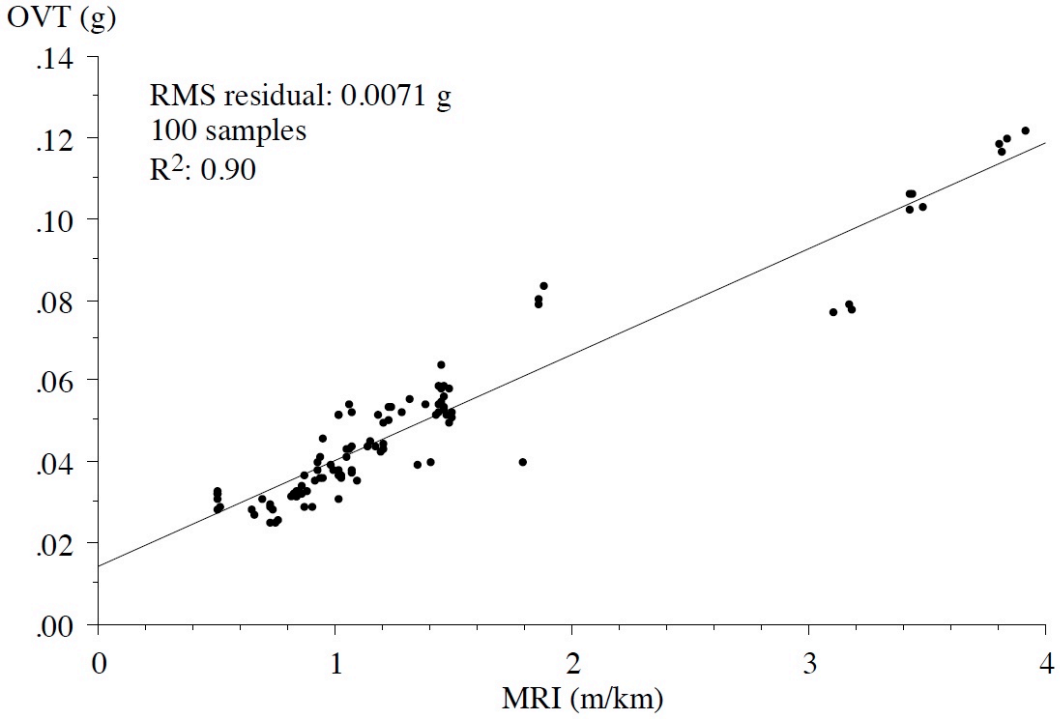

Figure B-4. OVT versus MRI, luxury SUV, 112-120 km/h.

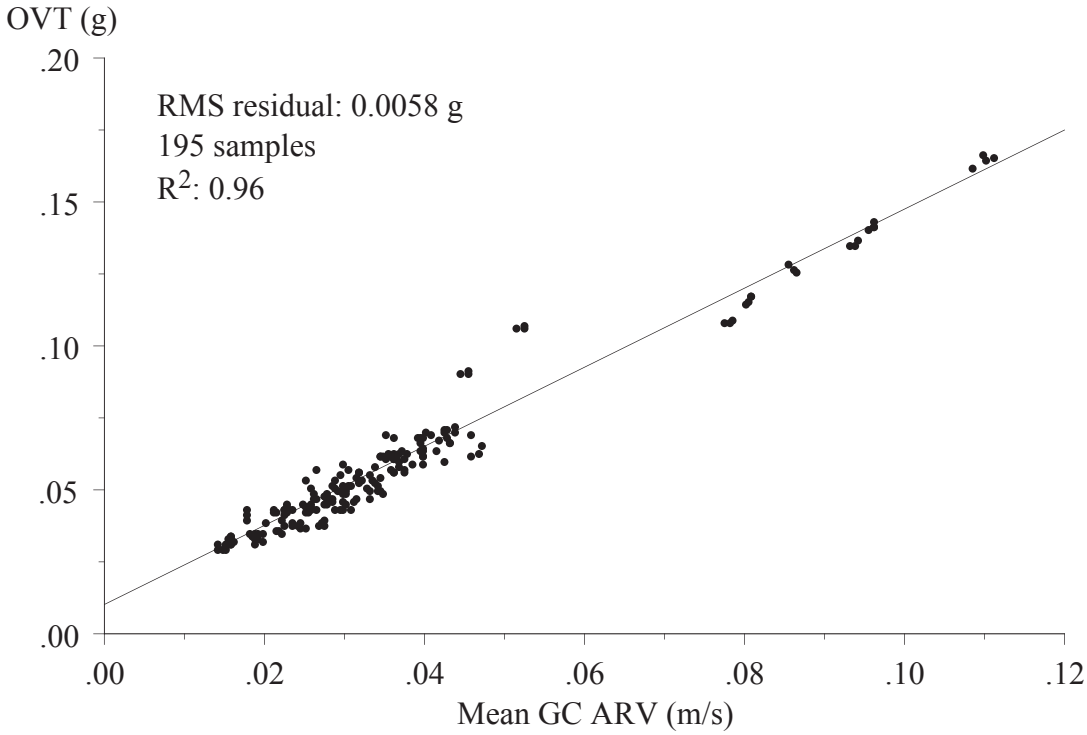

Figure B-5. OVT versus mean GC ARV, midsize sedan, 96-120 km/h.

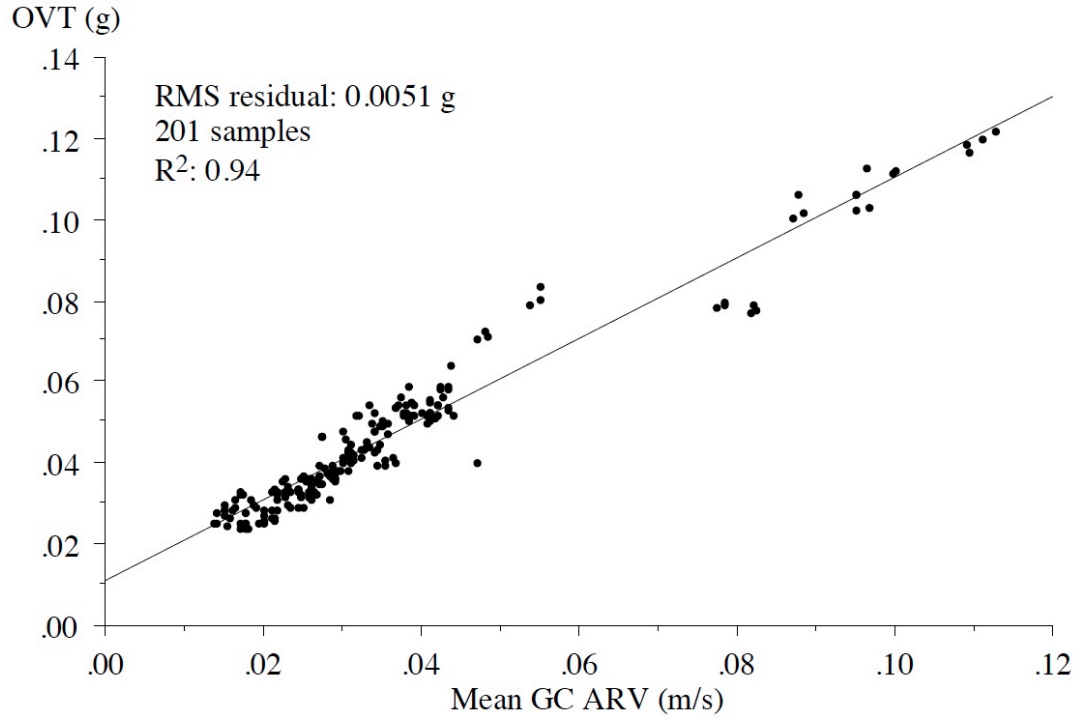

Figure B-6. OVT versus mean GC ARV, luxury SUV, 96-120 km/h.

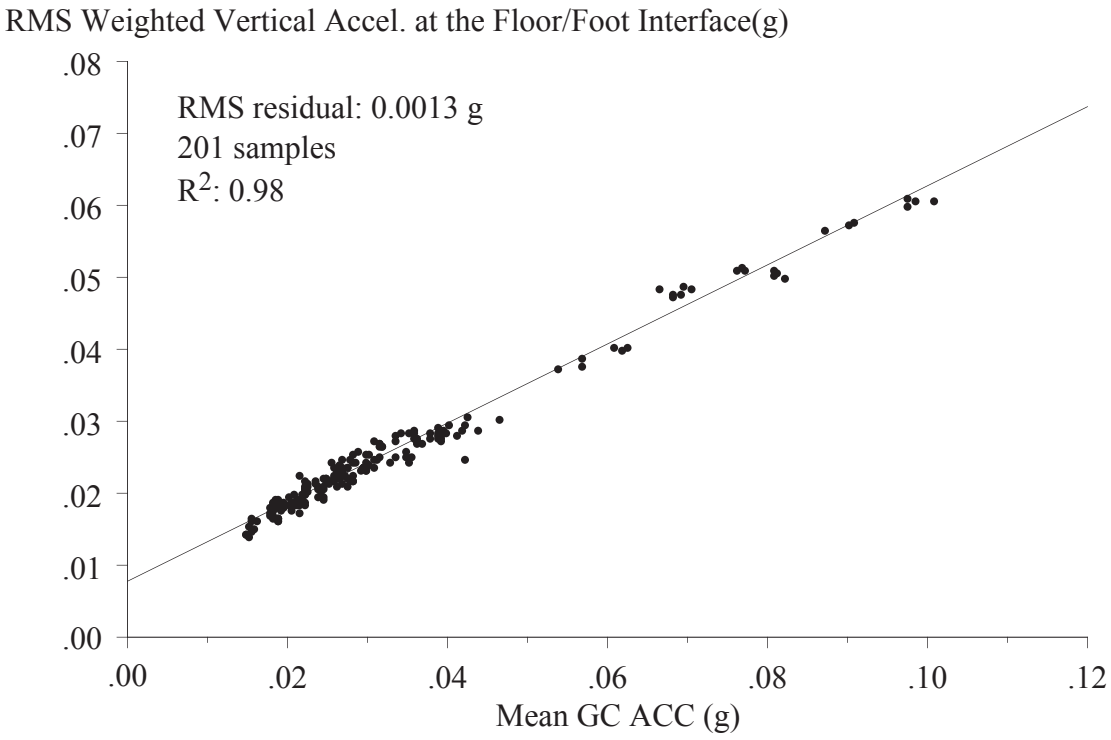

Figure B-7. Vertical floor/foot vibration versus mean GC ACC, luxury SUV, 96-120 km/h.